Lecture 5) Eigenstructure and Approximate Riemann Solvers for Hyperbolic Conservation Laws

By

Prof. Dinshaw S. Balsara (dbalsara@nd.edu)

Les Houches Summer School in Computational Astrophysics

http://www.nd.edu/~dbalsara/Numerical-PDE-Course

6.1) Introduction

Lecture 2 has shown us that *monotonicity preserving reconstruction* and Riemann solvers are important for linear hyperbolic equations. We studied the *eigenstructure* of the linear systems.

Lecture 3 has shown us the kinds of *simple waves -- shocks and rarefactions* -- that we get in a non-linear, scalar conservation law. We also got our first glimpse of an *approximate Riemann solver*.

Lecture 3 also showed that the same simple wave structures find analogues in systems of hyperbolic conservation laws. We described a *exact* and *approximate (two-shock) Riemann solvers*.

Here we study the eigenstructure of the Euler and MHD systems. The choice of these systems is based on utility. Rel. hydro & MHD are similar

First goal : ***Study eigenstructure*** for these systems. Different waves/discontinuities behave differently; can we understand them?

Exact Riemann solvers have been designed for all these systems. The barrier to their practical utilization in codes is *computational complexity*.

Much of the information generated by such Riemann solvers is *never used in* the computation of a *numerical flux*.

As the hyperbolic system gets larger, an increasing amount of information that is generated by the Riemann solver is discarded.

<u>Second Goal</u>: *Study linearized Riemann solvers*. These are approximate Riemann solvers.

What are the ***essential elements of any exact or approximate Riemann solver***?

1) A Self-Similar Wave Model. (Wave Model == how we conceptualize the waves in the Riemann solver. May not be the same as the exact RS.)

2) Consistency with the Conservation Law: Not just for infinitesimal fluctuations but also for isolated discontinuities of finite strength.

3) Entropy Enforcement: Arbitrary discontinuities to be resolved correctly. Need for conservation and entropy generation.

4) Preservation of Discontinities: Isolated contact discontinuities should not be smeared on the mesh. Shocks are self-steepening – ok to smear them. Contacts are not – must keep them intact as much as possible.

All of the Riemann Solvers discussed here are one dimensional. All multidimensional flow features are treated dimension-by-dimension. Imparts mesh imprinting.

Linearized (Approximate) Riemann Solvers: Try to turn $U_t + F(U)_x = 0$ into a suitable linear problem $U_t + \bar{A} U_x = 0$, $\bar{A}$ is a matrix. It is easy to study its eigenstructure. $\bar{A}(U_L, U_R)$ depends on both the input states!

A) When the difference between the left and right state is suitably small, can obtain : $\partial_t U + A \partial_x U = 0$ with $A \equiv \partial F(U)/\partial U$ i.e. problem linearizes easily $\Rightarrow$ consistency.

B) When left and right states differ by much, we _still_ want a matrix equation : $\partial_t U + \bar{A} \partial_x U = 0$ that mimics the above equation $\partial_t U + A \partial_x U = 0$.

C) The eigenstructure of $\bar{A}$ should have parallels to that of A in the linear regime. Question: What does this mean for eigenstructure? Relate it to linear systems (Lect 3).

D) When isolated discontinuities are present, the structure of $\bar{A}$ should be such that they can propagate at the "correct" speed. Question: What about self-similarity? Question: What does that give us? Can you relate it to what we learned in Chp 3?

Recall that the linearized Riemann solver preserves all isolated discontinuities exactly. Sometimes, we may not want to preserve all this structure.

In retrospect, the linearized RS is not positivity preserving; HLL RS is positivity preserving. Which is why we have several favorable variants of HLL.

The HLL Riemann solver, from Lect 3, is an example of such a Riemann solver that washes out some structure yet gives stability & positivity!

Linearized Riemann solvers can also be temperamental performers, especially in the vicinity of strong shocks. HLL Riemann solvers are robust and stable, so are its variants.

The variants of the HLL Riemann solver – HLLC, HLLI, HLLD – can even capture isolated discontinuities exactly.

Third goal: *Design HLL, HLLC, HLLI, LLF Riemann solvers and their variants for systems*.

6.2) The Eigenstructure of the Euler Equations

6.2.1) Derivation of the Eigensystem for the Euler Equations

Write the Euler equations as:

$$\partial_t U + \partial_x F(U) + \partial_y G(U) + \partial_z H(U) = 0$$

$$\frac{\partial}{\partial t} \begin{pmatrix} \rho \\ \rho\, v_x \\ \rho\, v_y \\ \rho\, v_z \\ \mathcal{E} \end{pmatrix} + \frac{\partial}{\partial x} \begin{pmatrix} \rho\, v_x \\ \rho\, v_x^2 + P \\ \rho\, v_x\, v_y \\ \rho\, v_x\, v_z \\ (\mathcal{E}+P)\, v_x \end{pmatrix} + \frac{\partial}{\partial y} \begin{pmatrix} \rho\, v_y \\ \rho\, v_x\, v_y \\ \rho\, v_y^2 + P \\ \rho\, v_y\, v_z \\ (\mathcal{E}+P)\, v_y \end{pmatrix} + \frac{\partial}{\partial z} \begin{pmatrix} \rho\, v_z \\ \rho\, v_x\, v_z \\ \rho\, v_y\, v_z \\ \rho\, v_z^2 + P \\ (\mathcal{E}+P)\, v_z \end{pmatrix} = 0$$

$$\mathcal{E} = e + \frac{1}{2} \rho\, \mathbf{v}^2 \qquad \text{with} \qquad e \equiv \frac{P}{\Gamma - 1}$$

Write the x-directional variation as: $\partial_t U + A\,\partial_x U = 0$ with $A \equiv \partial F(U)/\partial U$ given by

$$\frac{\partial}{\partial t}\begin{pmatrix}\rho \\ \rho\,v_x \\ \rho\,v_y \\ \rho\,v_z \\ \varepsilon\end{pmatrix} + \begin{pmatrix} 0 & 1 & 0 & 0 & 0 \\ -v_x^2 + \dfrac{(\Gamma-1)}{2}\,\mathbf{v}^2 & 2v_x - (\Gamma-1)\,v_x & -(\Gamma-1)\,v_y & -(\Gamma-1)\,v_z & (\Gamma-1) \\ -v_x v_y & v_y & v_x & 0 & 0 \\ -v_x v_z & v_z & 0 & v_x & 0 \\ -v_x H + \dfrac{(\Gamma-1)}{2}\,v_x\,\mathbf{v}^2 & H - (\Gamma-1)\,v_x^2 & -(\Gamma-1)\,v_x v_y & -(\Gamma-1)\,v_x v_z & \Gamma\,v_x \end{pmatrix} \frac{\partial}{\partial x}\begin{pmatrix}\rho \\ \rho\,v_x \\ \rho\,v_y \\ \rho\,v_z \\ \varepsilon\end{pmatrix} = 0$$

with the total enthalpy "H" defined by:

$$\rho\,H \equiv e + P + \frac{1}{2}\,\rho\,\mathbf{v}^2 \quad\Leftrightarrow\quad P = \frac{(\Gamma-1)}{\Gamma}\left[\rho\,H - \frac{1}{2}\,\rho\,\mathbf{v}^2\right] = (\Gamma-1)\left[\varepsilon - \frac{1}{2}\,\rho\,\mathbf{v}^2\right]$$

It is simpler to study this system in terms of the vector of primitive variables:

$$V \equiv \begin{pmatrix} \rho & v_x & v_y & v_z & P \end{pmatrix}^T$$

<u>Question</u>: If so, why do we still want to study the system in conservation form?

This is most easily done by recasting the system with the Jacobian matrices :

$\dfrac{\partial U}{\partial V}$ and $\dfrac{\partial V}{\partial U}$ (see text).

More familiar primitive form:

$$\frac{\partial}{\partial t}\begin{pmatrix} \rho \\ v_x \\ v_y \\ v_z \\ P \end{pmatrix} + \begin{pmatrix} v_x & \rho & 0 & 0 & 0 \\ 0 & v_x & 0 & 0 & 1/\rho \\ 0 & 0 & v_x & 0 & 0 \\ 0 & 0 & 0 & v_x & 0 \\ 0 & \Gamma P & 0 & 0 & v_x \end{pmatrix} \frac{\partial}{\partial x}\begin{pmatrix} \rho \\ v_x \\ v_y \\ v_z \\ P \end{pmatrix} = 0$$

Eigenvalues: $\{v_x - c_s, \quad v_x, \quad v_x, \quad v_x, \quad v_x + c_s\}$ where $c_s \equiv \sqrt{\dfrac{\Gamma P}{\rho}}$

Matrix of Right Eigenvectors:

$$R_p = \begin{pmatrix} 1 & 1 & 0 & 0 & 1 \\ -c_s/\rho & 0 & 0 & 0 & c_s/\rho \\ 0 & 0 & 1 & 0 & 0 \\ 0 & 0 & 0 & 1 & 0 \\ c_s^2 & 0 & 0 & 0 & c_s^2 \end{pmatrix}$$

Matrix of Orthonormal Left Eigenvectors:

$$L_p = \begin{pmatrix} 0 & -\rho/(2c_s) & 0 & 0 & 1/(2c_s^2) \\ 1 & 0 & 0 & 0 & -1/c_s \\ 0 & 0 & 1 & 0 & 0 \\ 0 & 0 & 0 & 1 & 0 \\ 0 & \rho/(2c_s) & 0 & 0 & 1/(2c_s^2) \end{pmatrix}$$

Question: Can you physically interpret the above eigenvectors?

6.3) Linearized Riemann Solver for the Euler Equations

Finding a linearization of the non-linear hyperbolic system is tantamount to saying that we want to replace $U_t + F(U)_x = 0$ by $\partial_t U + \bar{A} \, \partial_x U = 0$

Task: For general left & right states U_L and U_R, find a matrix $\bar{A}(U_L, U_R)$ such that:

(i) It is a linear mapping to the vector space "U" to the vector space "F".

(ii) As $U_L \to U_R \to U$, we have $\bar{A}(U_L, U_R) \to A(U)$. Yields consistency of flux.

(iii) For all U_L and U_R we have $\bar{A}(U_L, U_R) \, (U_R - U_L) = F(U_R) - F(U_L)$

Ensures that isolated discontinuities propagate at the right speed.

Let's see why:

Assume U_L and U_R are left and right states of an isolated discontinuity that moves with speed "S".

Nonlinear cons. law gives : $\quad F(U_R) - F(U_L) = S \, (U_R - U_L)$

Linearized system should give : $\quad \bar{A}(U_L, U_R) \, (U_R - U_L) = S \, (U_R - U_L)$

I.e. the two systems should predict the same propagation speed for the discontinuity.

This is ensured if : $\quad F(U_R) - F(U_L) = S \, (U_R - U_L) = \bar{A}(U_L, U_R) \, (U_R - U_L)$[11]

(iv) The eigenvectors of $\overline{A}\left(U_L, U_R\right)$ are linearly independent. $\Rightarrow$

Any jump $\left(U_R - U_L\right)$ can be projected into the eigenspace of $\overline{A}\left(U_L, U_R\right)$.

This is needed if we are to used methods drawn from linear hyp. systems in formulating a Riemann solver.

<u>Question</u>: How general can U_L and U_R be?

Collectively these four properties are known as "***Property U***", because they endow the Riemann solver with "uniform" validity at discontinuities.

Note that the linearized RS is not positivity preserving. So in principle, the (iv) property cannot *always* be guaranteed.

Even so, the linearized RS has some very desirable theoretical properties – it reduces dissipation to the minimum level that is allowed. That is why we continue to study it. The HLLI RS can reproduce this property of minimizing dissipation for intermediate waves.

There are many different ways to get Property U. Easiest approach is via *parameter vectors*:

$$W \equiv \left(w_1,\ w_2,\ w_3,\ w_4,\ w_5 \right)^T \equiv \rho^{1/2} \left(1,\ v_x,\ v_y,\ v_z,\ H \right)^T$$

$$\equiv \left(\sqrt{\rho},\ v_x \sqrt{\rho},\ v_y \sqrt{\rho},\ v_z \sqrt{\rho},\ H \sqrt{\rho} \right)^T$$

$$W_L \equiv \left(w_{1L},\ w_{2L},\ w_{3L},\ w_{4L},\ w_{5L} \right)^T \equiv \rho_L^{1/2} \left(1,\ v_{xL},\ v_{yL},\ v_{zL},\ H_L \right)^T$$

$$W_R \equiv \left(w_{1R},\ w_{2R},\ w_{3R},\ w_{4R},\ w_{5R} \right)^T \equiv \rho_R^{1/2} \left(1,\ v_{xR},\ v_{yR},\ v_{zR},\ H_R \right)^T$$

Recalling $\mathcal{E} = \dfrac{1}{\Gamma} \rho\, H + \dfrac{(\Gamma - 1)}{2\Gamma} \rho\, \mathbf{v}^2$, we can write the vectors "U" and "F" as:

$$U = \begin{pmatrix} \rho \\ \rho\, v_x \\ \rho\, v_y \\ \rho\, v_z \\ \mathcal{E} \end{pmatrix} = \begin{pmatrix} w_1^2 \\ w_1\, w_2 \\ w_1\, w_3 \\ w_1\, w_4 \\ \dfrac{1}{\Gamma} w_1\, w_5\ +\ \dfrac{(\Gamma - 1)}{2\Gamma} \left(w_2^2 + w_3^2 + w_4^2 \right) \end{pmatrix}$$

13

$$W \equiv \left(w_1, \ w_2, \ w_3, \ w_4, \ w_5\right)^T \equiv \rho^{1/2}\left(1, \ v_x, \ v_y, \ v_z, \ H\right)^T$$

$$\equiv \left(\sqrt{\rho}, \ v_x\sqrt{\rho}, \ v_y\sqrt{\rho}, \ v_z\sqrt{\rho}, \ H\sqrt{\rho}\right)^T$$

$$\rho H \equiv e + P + \frac{1}{2}\rho \mathbf{v}^2 \quad \Leftrightarrow \quad P = \frac{(\Gamma - 1)}{\Gamma}\left[\rho H - \frac{1}{2}\rho \mathbf{v}^2\right]$$

$$F = \begin{pmatrix} \rho v_x \\ \rho v_x^2 + P \\ \rho v_x v_y \\ \rho v_x v_z \\ \rho H v_x \end{pmatrix} = \begin{pmatrix} w_1 w_2 \\ \dfrac{(\Gamma - 1)}{\Gamma} w_1 w_5 \ + \ w_2^2 \ - \ \dfrac{(\Gamma - 1)}{2\Gamma}\left(w_2^2 + w_3^2 + w_4^2\right) \\ w_2 w_3 \\ w_2 w_4 \\ w_2 w_5 \end{pmatrix}$$

Notice that "U" and "F" are quadratic in the components of the parameter vectors.

Now realize the useful trick:

$$\Delta(p\,q) \equiv p_R\,q_R - p_L\,q_L = \frac{1}{2}(p_R + p_L)(q_R - q_L) + \frac{1}{2}(q_R + q_L)(p_R - p_L)$$

$$= \bar{p}\,\Delta q + \bar{q}\,\Delta p$$

where $\bar{p} \equiv \dfrac{1}{2}(p_R + p_L)$ and $\bar{q} \equiv \dfrac{1}{2}(q_R + q_L)$

From Calculus, recall that :- $d(p\,q) = p\,dq + q\,dp$ ← See the analogy?

We also define the *Roe - averaged variables* :

$$\bar{v}_x \equiv \frac{\bar{w}_2}{\bar{w}_1} = \frac{\sqrt{\rho_L}\,v_{xL} + \sqrt{\rho_R}\,v_{xR}}{\sqrt{\rho_L} + \sqrt{\rho_R}} \;\; ; \;\; \bar{v}_y \equiv \frac{\bar{w}_3}{\bar{w}_1} \;\; ; \;\; \bar{v}_z \equiv \frac{\bar{w}_4}{\bar{w}_1} \;\; ; \;\; \bar{H} \equiv \frac{\bar{w}_5}{\bar{w}_1} \;\; ;$$

$$\rho^* \equiv \sqrt{\rho_L \rho_R}$$

These variables enable us to represent $(U_R - U_L)$ and $(F_R - F_L)$ in terms of $(W_R - W_L)$.

Let us see how it is done.

$$U = \begin{pmatrix} \rho \\ \rho\, v_x \\ \rho\, v_y \\ \rho\, v_z \\ \varepsilon \end{pmatrix} = \begin{pmatrix} w_1^2 \\ w_1\, w_2 \\ w_1\, w_3 \\ w_1\, w_4 \\ \dfrac{1}{\Gamma} w_1\, w_5 \; + \; \dfrac{(\Gamma - 1)}{2\Gamma}\left(w_2^2 + w_3^2 + w_4^2 \right) \end{pmatrix}$$

$$U_R - U_L = \bar{B}\left(W_R - W_L \right) = \begin{pmatrix} 2\bar{w}_1 & 0 & 0 & 0 & 0 \\ \bar{w}_2 & \bar{w}_1 & 0 & 0 & 0 \\ \bar{w}_3 & 0 & \bar{w}_1 & 0 & 0 \\ \bar{w}_4 & 0 & 0 & \bar{w}_1 & 0 \\ \dfrac{1}{\Gamma}\bar{w}_5 & \dfrac{\Gamma - 1}{\Gamma}\bar{w}_2 & \dfrac{\Gamma - 1}{\Gamma}\bar{w}_3 & \dfrac{\Gamma - 1}{\Gamma}\bar{w}_4 & \dfrac{1}{\Gamma}\bar{w}_1 \end{pmatrix} \left(W_R - W_L \right)$$

It is also useful to write :- $\left(W_R - W_L \right) = \left(\bar{B} \right)^{-1} \left(U_R - U_L \right)$

$$U_R - U_L = \overline{B}\left(W_R - W_L\right) = \begin{pmatrix} 2\overline{w}_1 & 0 & 0 & 0 & 0 \\ \overline{w}_2 & \overline{w}_1 & 0 & 0 & 0 \\ \overline{w}_3 & 0 & \overline{w}_1 & 0 & 0 \\ \overline{w}_4 & 0 & 0 & \overline{w}_1 & 0 \\ \dfrac{1}{\Gamma}\overline{w}_5 & \dfrac{\Gamma-1}{\Gamma}\overline{w}_2 & \dfrac{\Gamma-1}{\Gamma}\overline{w}_3 & \dfrac{\Gamma-1}{\Gamma}\overline{w}_4 & \dfrac{1}{\Gamma}\overline{w}_1 \end{pmatrix}\left(W_R - W_L\right)$$

$$= \overline{w}_1 \begin{pmatrix} 2 & 0 & 0 & 0 & 0 \\ \overline{v}_x & 1 & 0 & 0 & 0 \\ \overline{v}_y & 0 & 1 & 0 & 0 \\ \overline{v}_z & 0 & 0 & 1 & 0 \\ \dfrac{1}{\Gamma}\overline{H} & \dfrac{\Gamma-1}{\Gamma}\overline{v}_x & \dfrac{\Gamma-1}{\Gamma}\overline{v}_y & \dfrac{\Gamma-1}{\Gamma}\overline{v}_z & \dfrac{1}{\Gamma} \end{pmatrix}\left(W_R - W_L\right)$$

This defines the matrix $\overline{B}$. Notice that $\overline{B}$ is lower triangular, therefore, it is easy to invert.

$$F_R - F_L = \bar{C}\,(W_R - W_L) = \begin{pmatrix} \bar{w}_2 & \bar{w}_1 & 0 & 0 & 0 \\ \dfrac{\Gamma-1}{\Gamma}\bar{w}_5 & \dfrac{\Gamma+1}{\Gamma}\bar{w}_2 & -\dfrac{\Gamma-1}{\Gamma}\bar{w}_3 & -\dfrac{\Gamma-1}{\Gamma}\bar{w}_4 & \dfrac{\Gamma-1}{\Gamma}\bar{w}_1 \\ 0 & \bar{w}_3 & \bar{w}_2 & 0 & 0 \\ 0 & \bar{w}_4 & 0 & \bar{w}_2 & 0 \\ 0 & \bar{w}_5 & 0 & 0 & \bar{w}_2 \end{pmatrix} (W_R - W_L)$$

$$= \bar{w}_1 \begin{pmatrix} \bar{v}_x & 1 & 0 & 0 & 0 \\ \dfrac{\Gamma-1}{\Gamma}\bar{H} & \dfrac{\Gamma+1}{\Gamma}\bar{v}_x & -\dfrac{\Gamma-1}{\Gamma}\bar{v}_y & -\dfrac{\Gamma-1}{\Gamma}\bar{v}_z & \dfrac{\Gamma-1}{\Gamma} \\ 0 & \bar{v}_y & \bar{v}_x & 0 & 0 \\ 0 & \bar{v}_z & 0 & \bar{v}_x & 0 \\ 0 & \bar{H} & 0 & 0 & \bar{v}_x \end{pmatrix} (W_R - W_L)$$

This defines the matrix $\bar{C}$.

From the previous page, recall that :- $(W_R - W_L) = (\bar{B})^{-1}(U_R - U_L)$

We then have from this page that :- $F_R - F_L = \bar{C}\,(W_R - W_L) = \bar{C}\,(\bar{B})^{-1}\,(U_R - U_L)$

This enables us to identify : $\bar{A}(U_R, U_L) \equiv \bar{C}\,(\bar{B})^{-1}$

$$\bar{A}\left(U_L, U_R\right) = \bar{C}\left(\bar{B}\right)^{-1} = \begin{pmatrix} 0 & 1 & 0 & 0 & 0 \\ -\bar{v}_x^2 + \dfrac{(\Gamma-1)}{2}\,\bar{\mathbf{v}}^2 & 2\bar{v}_x - (\Gamma-1)\bar{v}_x & -(\Gamma-1)\bar{v}_y & -(\Gamma-1)\bar{v}_z & (\Gamma-1) \\ -\bar{v}_x\bar{v}_y & \bar{v}_y & \bar{v}_x & 0 & 0 \\ -\bar{v}_x\bar{v}_z & \bar{v}_z & 0 & \bar{v}_x & 0 \\ -\bar{v}_x\bar{H} + \dfrac{(\Gamma-1)}{2}\,\bar{v}_x\,\bar{\mathbf{v}}^2 & \bar{H} - (\Gamma-1)\bar{v}_x^2 & -(\Gamma-1)\bar{v}_x\bar{v}_y & -(\Gamma-1)\bar{v}_x\bar{v}_z & \Gamma\,\bar{v}_x \end{pmatrix}$$

The *amazing fact* is that this matrix is formally just the same as the original characteristic matrix!!

We have no reason to expect this, since the variables in the above matrix have no physical standing; they only have a formal standing.

We make the connection more concrete by defining : $\bar{P} \equiv \dfrac{(\Gamma-1)}{\Gamma}\,\rho^* \left[\bar{H} - \dfrac{1}{2}\left(\bar{v}_x^2 + \bar{v}_y^2 + \bar{v}_z^2\right)\right]$

Recall that physically speaking we indeed do have : $P = \dfrac{(\Gamma-1)}{\Gamma}\rho\left[H - \dfrac{1}{2}\mathbf{v}^2\right]$

We can thus express the eigenvalues of the above matrix as:

$$\left\{\bar{v}_x - \bar{c}_s,\quad \bar{v}_x,\quad \bar{v}_x,\quad \bar{v}_x,\quad \bar{v}_x + \bar{c}_s\right\} \quad \text{where } \bar{c}_s^2 \equiv \dfrac{\Gamma\,\bar{P}}{\rho^*}$$

This exact, formal analogy can be used to derive the eigenvectors too. We just make the formal transcriptions:

$$\rho \rightarrow \rho^* \;\; ; \;\; v_x \rightarrow \overline{v}_x \;\; ; \;\; v_y \rightarrow \overline{v}_y \;\; ; \;\; v_z \rightarrow \overline{v}_z \;\; ; \;\; H \rightarrow \overline{H} \;\; ; \;\; c_s \rightarrow \overline{c}_s$$

Notice two important points of difference:

A) If U_L and U_R correspond to the exact jump in a right-going shock then $\overline{v}_x + \overline{c}_s$ is the right-going shock speed. One cannot say the same about $v_x + c_s$.

B) For any physical state, P is guaranteed to be positive.
We can't guarantee positivity of $\overline{P}$ for any two physical states U_L and U_R.

Notice too that nothing has been said so far on the *entropy fix*. From the discussion in Lecture 3, we know that we must have an entropy fix.

The linearized Riemann solver has also been formulated for *real gases*.

6.4) Entropy Fixes for Linearized Riemann Solvers

By linearizing a non-linear system of conservation laws, we wish to replace the non-linear system with an equivalent linear system. We have studied linear hyperbolic systems. We, therefore, wish to draw upon insights from that study in Section 3.4.

Having obtained an $M \times M$ matrix $\overline{A}\left(U_L, U_R\right)$, we perform its characteristic analysis:
I.e. we obtain $\left\{\overline{\lambda}^m : m = 1, ..., M\right\}$, $\left\{\overline{l}^m : m = 1, ..., M\right\}$, $\left\{\overline{r}^m : m = 1, ..., M\right\}$.

Given any arbitrary jump across a zone boundary $\left(U_R - U_L\right)$, we can project it onto the space of right eigenvectors:

$$U_R - U_L = \sum_{m=1}^{M} \alpha^m \, \overline{r}^m \quad \text{where} \quad \alpha^m \equiv \overline{l}^m \bullet \left(U_R - U_L\right)$$

This just represents each *simple wave discontinuity* as a discrete jump in the solution without examining whether it is a physical *compressive shock* or an unphysical *rarefaction shock*. It is up to us to go back and provide an *entropy fix* to the rarefaction shocks.

As with linear hyperbolic systems, we get $M+1$ constant states in space-time:

$$U(x,t) = U_L \qquad\qquad\qquad\qquad\qquad\qquad\qquad \text{for } \frac{x}{t} < \bar{\lambda}^1$$

$$= U^{(m)} \equiv U_L + \sum_{p=1}^{m} \alpha^p \, \bar{r}^p = U_R - \sum_{p=m+1}^{M} \alpha^p \, \bar{r}^p \quad \text{for } \bar{\lambda}^m < \frac{x}{t} < \bar{\lambda}^{m+1} \;\; , \;\; m=1,...,M-1$$

$$= U_R \qquad\qquad\qquad\qquad\qquad\qquad\qquad \text{for } \bar{\lambda}^M < \frac{x}{t}$$

And their associated fluxes:

$$F(x,t) = F_L \qquad\qquad\qquad\qquad\qquad\qquad\qquad \text{for } \frac{x}{t} < \bar{\lambda}^1$$

$$= F^{(m)} \equiv F_L + \sum_{p=1}^{m} \bar{\lambda}^p \alpha^p \, \bar{r}^p = F_R - \sum_{p=m+1}^{M} \bar{\lambda}^p \alpha^p \, \bar{r}^p \quad \text{for } \bar{\lambda}^m < \frac{x}{t} < \bar{\lambda}^{m+1} \;\; , \;\; m=1,...,M-1$$

$$= F_R \qquad\qquad\qquad\qquad\qquad\qquad\qquad \text{for } \bar{\lambda}^M < \frac{x}{t}$$

Find m_0 such that:

$$\bar{\lambda}^{m_0} < 0 \leq \bar{\lambda}^{m_0+1}$$
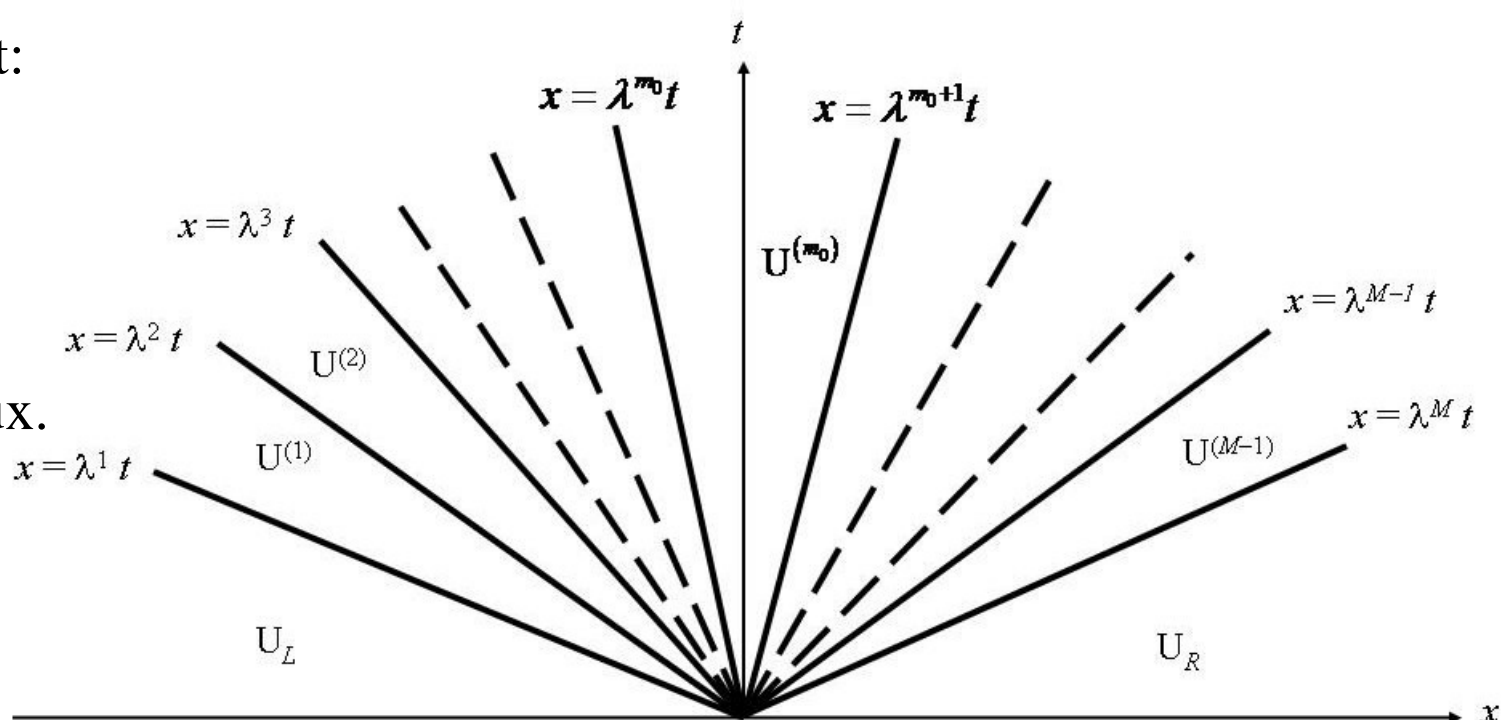
m_0 helps us find resolved state and numerical flux.

Fig. 3.10 shows the space-time diagram for the propagation of finite amplitude (or infinitesimal) perturbations for an M-component linear hyperbolic system. The solid lines show waves; the dashed lines represent the presence of further waves that may not be explicitly shown here. The left and right states are denoted by U_L and U_R. The resolved state of the Riemann problem is shown as $U^{(RS)} \equiv U^{(m_0)}$.

To apply an entropy fix, find the three states $U^{(m_0-1)}$, $U^{(m_0)}$ and $U^{(m_0+1)}$. Whether or not an entropy fix is needed is decided by examining wave speeds in those three states, as shown next.

23

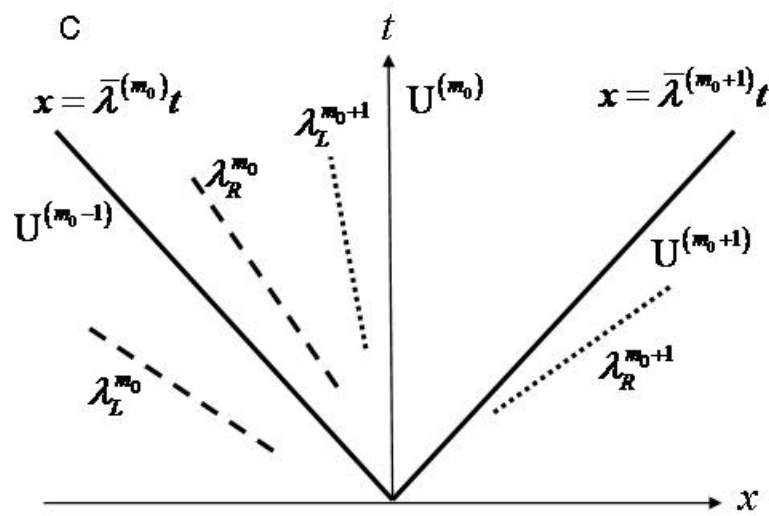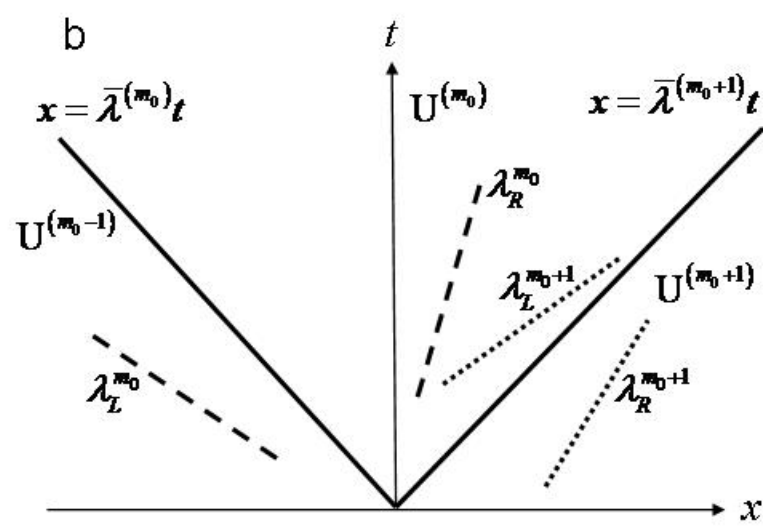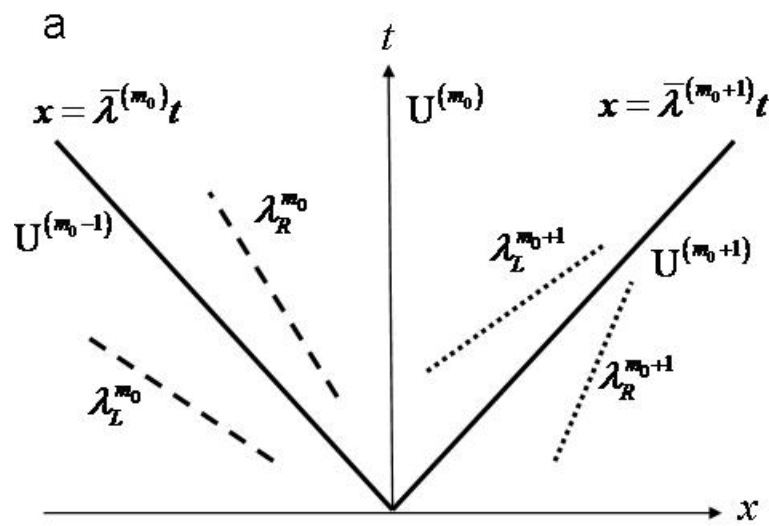**a** — panel showing t vs x axes, with $x = \bar{\lambda}^{(m_0)}t$, $U^{(m_0)}$, $x = \bar{\lambda}^{(m_0+1)}t$, $U^{(m_0-1)}$, $\lambda_R^{m_0}$, $\lambda_L^{m_0+1}$, $U^{(m_0+1)}$, $\lambda_R^{m_0+1}$, $\lambda_L^{m_0}$

b — panel showing t vs x axes, with $x = \bar{\lambda}^{(m_0)}t$, $U^{(m_0)}$, $x = \bar{\lambda}^{(m_0+1)}t$, $U^{(m_0-1)}$, $\lambda_R^{m_0}$, $\lambda_L^{m_0+1}$, $U^{(m_0+1)}$, $\lambda_R^{m_0+1}$, $\lambda_L^{m_0}$

c — panel showing t vs x axes, with $x = \bar{\lambda}^{(m_0)}t$, $\lambda_L^{m_0+1}$, $U^{(m_0)}$, $x = \bar{\lambda}^{(m_0+1)}t$, $\lambda_R^{m_0}$, $U^{(m_0-1)}$, $U^{(m_0+1)}$, $\lambda_L^{m_0}$, $\lambda_R^{m_0+1}$

Fig. 6.1 Shows the different situations that may prevail when a linearized Riemann solver is used. The characteristics of the m_0^{th} family are shown as dashed lines; those of the $(m_0+1)^{th}$ family are shown as dotted lines. The other wave families are not shown. No entropy fix is needed in Fig. 6.1a. The m_0^{th} wave in Fig. 6.1b needs an entropy fix. The $(m_0+1)^{th}$ wave in Fig. 6.1c needs an entropy fix.

We only show the characteristics associated with the m_0 and m_0+1 wave families.

Questions: Which of these waves is a shock, which of them are rarefactions?

Which of of the wave families in each panel need an entropy fix? Assume non-moving boundaries.

24

Further caveats:

(i) Examine the resolved states for positivity, linearized Riemann solvers have problems when it comes to maintaining positivity.

(ii) One usually uses a shortcut by defining $\lambda_L^{m_0} \equiv \lambda^{m_0}\left(U_L\right)$ and $\lambda_R^{m_0} \equiv \lambda^{m_0}\left(U_R\right)$ and using the condition $\lambda_L^{m_0} < 0 < \lambda_R^{m_0}$ to identify the formation of a rarefaction fan in the m_0^{th} wave family.

We provide two entropy fixes:

Entropy Fix # 1:

If $\lambda_L^{m_0} < 0 < \lambda_R^{m_0}$ our resolved flux should be a linear combination of the fluxes $F^{(m_0-1)}$ and $F^{(m_0)}$.

Here we have $F^{(m_0)} = F^{(m_0-1)} + \bar{\lambda}^{m_0} \alpha^{m_0} \bar{r}^{m_0}$ so that the full contribution from the m_0^{th} wave family is $\bar{\lambda}^{m_0} \alpha^{m_0} \bar{r}^{m_0}$.

With $0<\beta<1$, let the contribution from the left of the zone boundary be : $\beta \, \lambda_L^{m_0} \alpha^{m_0} \, \overline{r}^{m_0}$

Similarly, let the contribution from the right of the zone boundary be : $(1-\beta) \, \lambda_R^{m_0} \alpha^{m_0} \, \overline{r}^{m_0}$

The two contributions should add up to the full contribution that we identified before:

$$\beta \, \lambda_L^{m_0} \alpha^{m_0} \, \overline{r}^{m_0} + (1-\beta) \, \lambda_R^{m_0} \alpha^{m_0} \, \overline{r}^{m_0} = \overline{\lambda}^{m_0} \alpha^{m_0} \, \overline{r}^{m_0}$$

so that:

$$\beta = \frac{\lambda_R^{m_0} - \overline{\lambda}^{m_0}}{\lambda_R^{m_0} - \lambda_L^{m_0}}$$

With the above definition, and several other ancillary definitions (see below), we are ready to obtain closed form expressions for the conserved variables and fluxes.

When $\lambda_L^m \, \lambda_R^m \geq 0$, we make the following definitions:-

$$\lambda^{+,m} \equiv \max\left(\overline{\lambda}^m, 0\right) \; ; \; \lambda^{-,m} \equiv \min\left(\overline{\lambda}^m, 0\right) \; ; \; \alpha^{+,m} \equiv \alpha^m \mathrm{H}\left(\overline{\lambda}^m\right) \; ; \; \alpha^{-,m} \equiv \alpha^m \mathrm{H}\left(-\overline{\lambda}^m\right)$$

When $\lambda_L^m \, \lambda_R^m < 0$, we make the following definitions:-

$$\lambda^{+,m} \equiv \frac{\overline{\lambda}^m - \lambda_L^m}{\lambda_R^m - \lambda_L^m} \lambda_R^m \; ; \; \lambda^{-,m} \equiv \frac{\lambda_R^m - \overline{\lambda}^m}{\lambda_R^m - \lambda_L^m} \lambda_L^m \; ; \; \alpha^{+,m} \equiv \frac{\overline{\lambda}^m - \lambda_L^m}{\lambda_R^m - \lambda_L^m} \alpha^m \; ; \; \alpha^{-,m} \equiv \frac{\lambda_R^m - \overline{\lambda}^m}{\lambda_R^m - \lambda_L^m} \alpha^m$$

Where we also define:- $\left|\lambda^m\right| \equiv \lambda^{+,m} - \lambda^{-,m}$

$$U_{\text{lin}}^{(RS)} = U_L + \sum_{m=1}^{M} \alpha^{-,m} \, \overline{r}^m$$

$$= U_R - \sum_{m=1}^{M} \alpha^{+,m} \, \overline{r}^m$$

$$= \frac{1}{2}\left(U_R + U_L\right) - \frac{1}{2}\sum_{m=1}^{M} \left(\alpha^{+,m} - \alpha^{-,m}\right) \overline{r}^m$$

$$F_{\text{lin}}^{(RS)} = F_L + \sum_{m=1}^{M} \lambda^{-,m} \, \alpha^m \, \overline{r}^m = F_L + A^-\left(U_R - U_L\right)$$

$$= F_R - \sum_{m=1}^{M} \lambda^{+,m} \, \alpha^m \, \overline{r}^m = F_R - A^+\left(U_R - U_L\right)$$

$$= \frac{1}{2}\left(F_R + F_L\right) - \frac{1}{2}\sum_{m=1}^{M} \left|\lambda^m\right| \alpha^m \, \overline{r}^m = \frac{1}{2}\left(F_R + F_L\right) - \frac{1}{2}\left|A\right|\left(U_R - U_L\right)$$

This is very reminiscent of the linear case, except that the above definitions build in the entropy fix. The book provides further detail.

All is not perfect with linearized Riemann solvers:

High speed flows can be especially problematical. <u>Question</u>: Why?

We have a need for *positively conservative* schemes, i.e. schemes that can guarantee that the pressure and density remain non-negative.

The <u>linearized Riemann solver is not positively conservative</u>. <u>HLL is</u>. The states in the next figure can cause a linearized Riemann solver to choke!
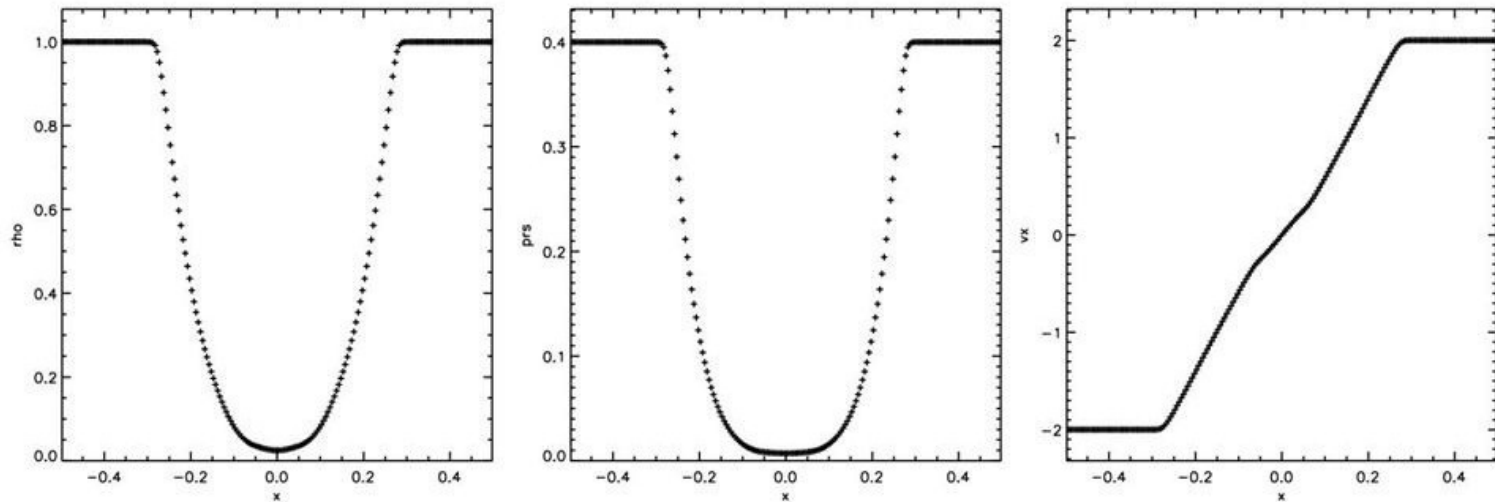
This figure shows the density, pressure and x-velocity from a Riemann problem with a strong rarefaction. The density and pressure reach values that are almost close to zero. Note though that negative densities and pressures do not arise.

They are also susceptible to a *carbuncle instability* when strong shocks move slowly relative to the mesh.
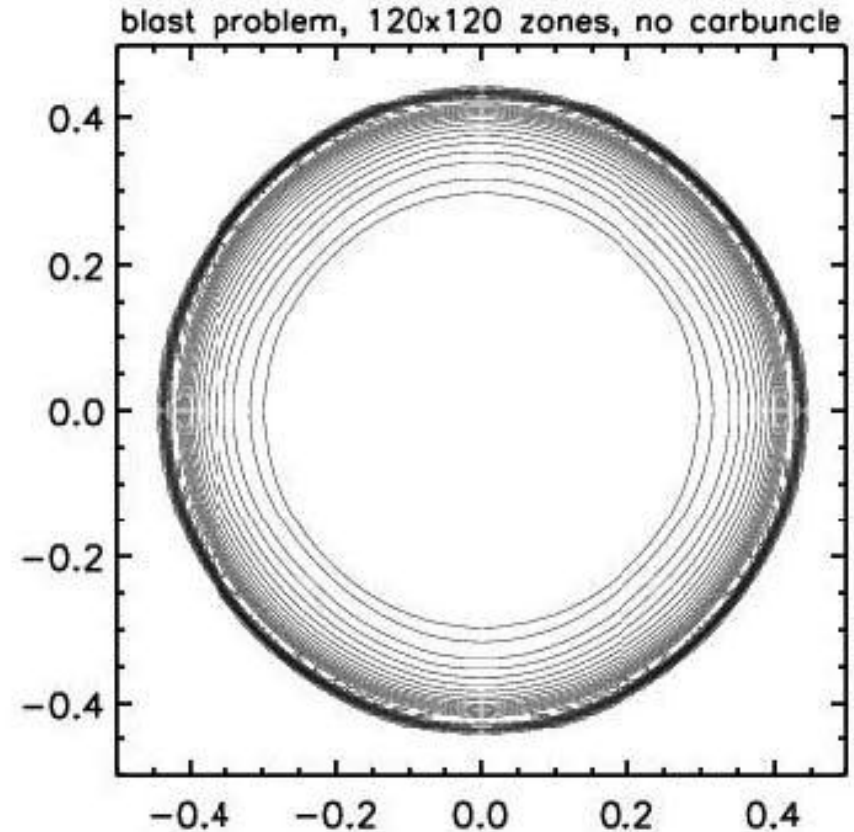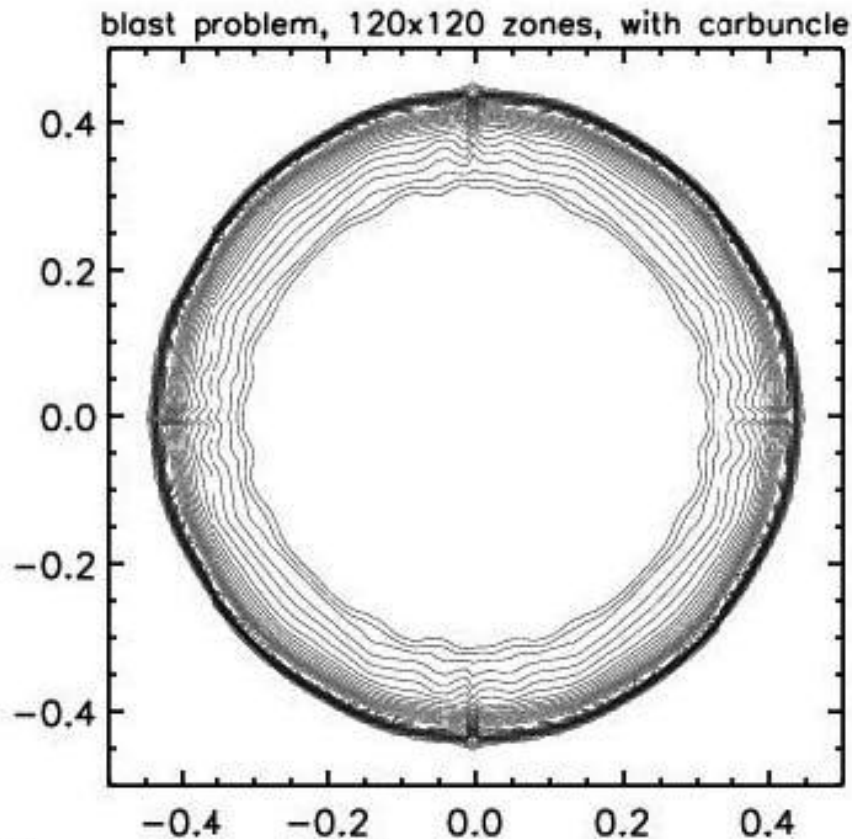
Strong blast problem in two dimensions. The left panel shows the formation of the carbuncle when a dimensionally split scheme with a linearized Riemann solver was used. The right panel does not show a carbuncle because a dimensionally unsplit scheme with an HLL fix to the linearized Riemann solver was used.

6.5) HLL, HLLC and HLLI Riemann Solvers

Consider the states in the hydrodynamical Riemann problem, shown below.

Below we also show the simplifications in the *wave model* that are made for the ***HLL and HLLC Riemann solvers***.
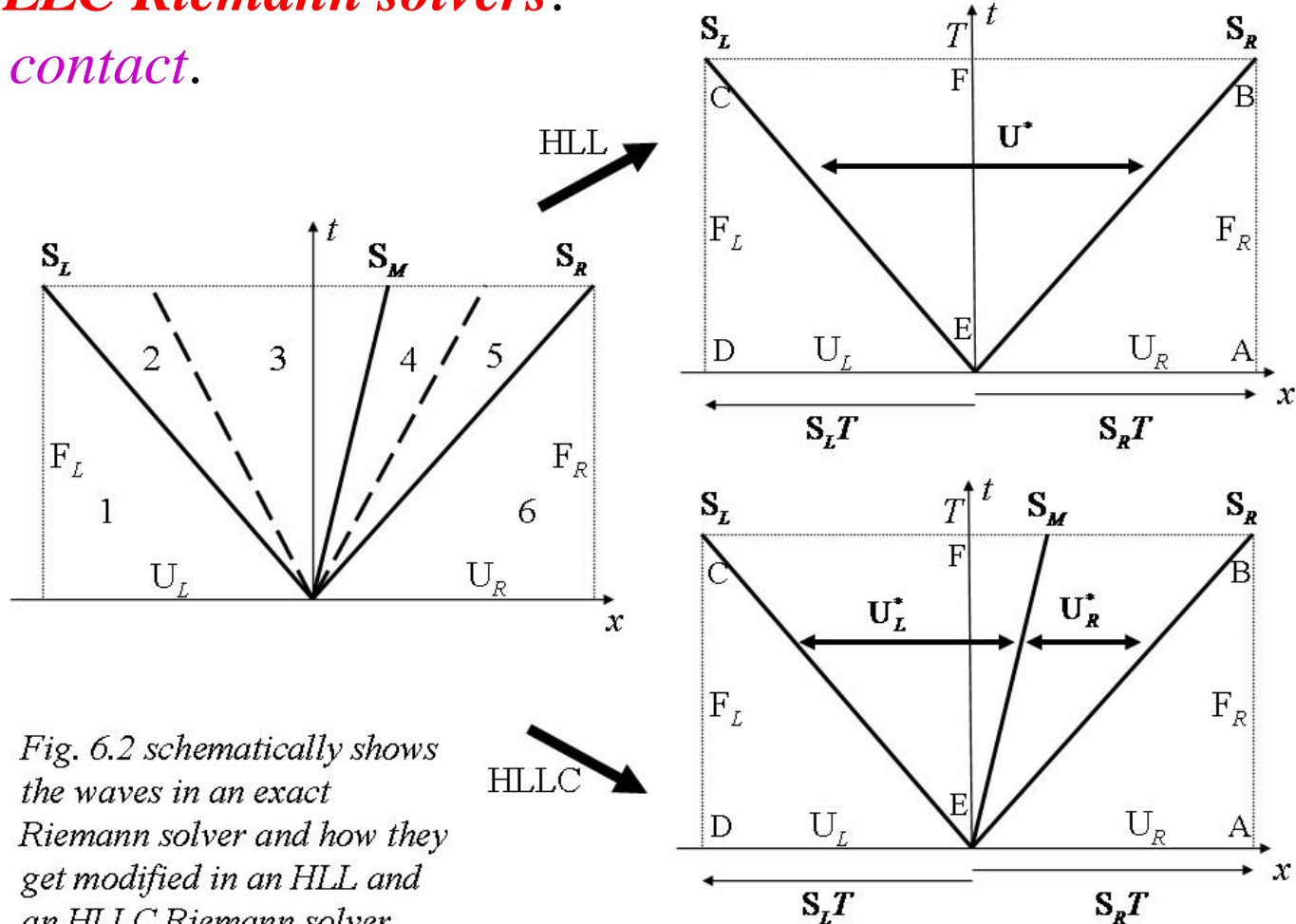The "C" stands for *contact*.

Fig. 6.2 schematically shows the waves in an exact Riemann solver and how they get modified in an HLL and an HLLC Riemann solver.

6.5.1) HLL Riemann Solver

Question: For the scalar conservation law, which structure did the wave model of the HLL Riemann solver average over?

Question: If we make a similar wave model for the Euler equations, which structures are we averaging over?

$$U_{HLL}^{(RS)} = \begin{cases} U_L & \text{if } S_L > 0 \\ U^* & \text{if } S_L \leq 0 \leq S_R \\ U_R & \text{if } S_R < 0 \end{cases} \quad \text{with} \quad U^* = \frac{S_R\, U_R - S_L\, U_L - \left(F_R - F_L \right)}{S_R - S_L}$$

$$F_{HLL}^{(RS)} = \begin{cases} F_L & \text{if } S_L > 0 \\ F^* & \text{if } S_L \leq 0 \leq S_R \\ F_R & \text{if } S_R < 0 \end{cases}$$

$$\text{with} \quad F^* = \left[\frac{S_R}{S_R - S_L} \right] F_L - \left[\frac{S_L}{S_R - S_L} \right] F_R + \left[\frac{S_R\, S_L}{S_R - S_L} \right] \left(U_R - U_L \right)$$

$$\text{and} \quad S_L \equiv \min\left(\lambda^1\left(U_L \right), \overline{v}_x - \overline{c}_s \right) \quad ; \quad S_R \equiv \max\left(\lambda^M\left(U_R \right), \overline{v}_x + \overline{c}_s \right)$$

For a scalar conservation law, we have no further requirements. For Euler equations, we would make some further demands:

1) Notice that if we have an isolated right-going shock, the HLL Riemann solver *picks out the correct flux*.
<u>Question</u>: For a transonic shock (with $S_L < 0 < S_R$) this is non-trivial. Can you prove it?

2) For open rarefaction fans that straddle the zone boundary, the *entropy fix* is also naturally built in.

3) The HLL Riemann solver also maintains positivity of the resolved state U^*. A result from Einfeldt et al (1991) then claims that a scheme that uses such a Riemann solver will also *keep the pressure positive*. This guarantee is only true in 1D; it does not extend to 2D and 3D.

6.5.2) HLLC Riemann Solver (Philosophy:- Start with HLL & build on top of it.)

The HLLC Riemann solver is designed to overcome the one failing of the HLL Riemann solver – the inability to capture *contact discontinuities*.

The resolution is to put two constant states between the left and right states that are separated by a contact discontinuity moving with a speed S_M. This is an *improvement of our wave model*.

$$U_{\text{HLLC}}^{(RS)} = \begin{cases} U_L & \text{if } S_L > 0 \\ U_L^* & \text{if } S_L \leq 0 \leq S_M \\ U_R^* & \text{if } S_M \leq 0 \leq S_R \\ U_R & \text{if } S_R < 0 \end{cases} \qquad F_{\text{HLLC}}^{(RS)} = \begin{cases} F_L & \text{if } S_L > 0 \\ F_L^* & \text{if } S_L \leq 0 \leq S_M \\ F_R^* & \text{if } S_M \leq 0 \leq S_R \\ F_R & \text{if } S_R < 0 \end{cases}$$

For the contact discontinuity to have the properties of an actual contact discontinuity, we demand:

$$S_M = v_{xL}^* = v_{xR}^* = v_x^*$$

Question: But how do we obtain S_M ? Answer: Use the components of U^* from the HLL Riemann solver.

$$S_M = v^*_{xL} = v^*_{xR} = v^*_x = \frac{U^*_2}{U^*_1} = \frac{\rho_R \, v_{xR} \left(S_R - v_{xR} \right) - \rho_L \, v_{xL} \left(S_L - v_{xL} \right) + P_L - P_R}{\rho_R \left(S_R - v_{xR} \right) - \rho_L \left(S_L - v_{xL} \right)}$$

A *pleasant corollary* of making this choice is that the pressure P^* is a constant across the contact. I.e. P^* is the same in U^*_L and U^*_R .

Question: But how do we obtain the post-shock states, U^*_L and U^*_R ?

Answer: Jump conditions at discontinuities:

Left: $F^*_L - F_L = S_L \left(U^*_L - U_L \right)$

$\Leftrightarrow \quad S_L U^*_L - F^*_L = S_L U_L - F_L$

Right: $F^*_R - F_R = S_R \left(U^*_R - U_R \right)$

$\Leftrightarrow \quad S_R U^*_R - F^*_R = S_R U_R - F_R$
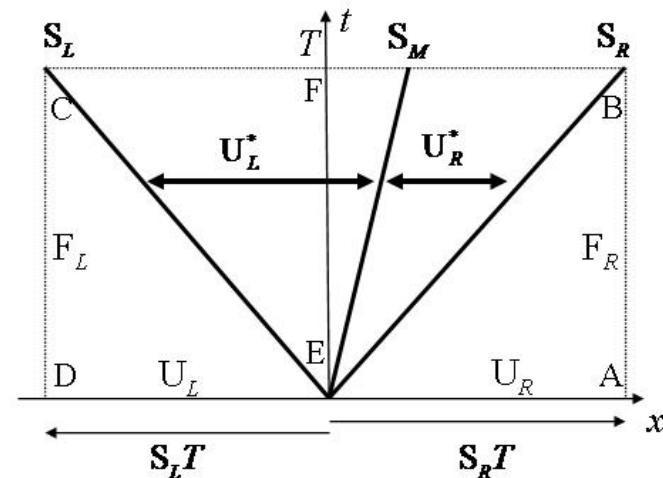
Left:

$$
S_L \begin{pmatrix} \rho_L^* \\ \rho_L^* S_M \\ \rho_L^* v_{yL}^* \\ \rho_L^* v_{zL}^* \\ \mathcal{E}_L^* \end{pmatrix} - \begin{pmatrix} \rho_L^* S_M \\ \rho_L^* S_M^2 + P_L^* \\ \rho_L^* S_M v_{yL}^* \\ \rho_L^* S_M v_{zL}^* \\ (\mathcal{E}_L^* + P_L^*) S_M \end{pmatrix} = S_L \begin{pmatrix} \rho_L \\ \rho_L v_{xL} \\ \rho_L v_{yL} \\ \rho_L v_{zL} \\ \mathcal{E}_L \end{pmatrix} - \begin{pmatrix} \rho_L v_{xL} \\ \rho_L v_{xL} v_{xL} + P_L \\ \rho_L v_{xL} v_{yL} \\ \rho_L v_{xL} v_{zL} \\ (\mathcal{E}_L + P_L) v_{xL} \end{pmatrix}
$$

Right:

$$
S_R \begin{pmatrix} \rho_R^* \\ \rho_R^* S_M \\ \rho_R^* v_{yR}^* \\ \rho_R^* v_{zR}^* \\ \mathcal{E}_R^* \end{pmatrix} - \begin{pmatrix} \rho_R^* S_M \\ \rho_R^* S_M^2 + P_R^* \\ \rho_R^* S_M v_{yR}^* \\ \rho_R^* S_M v_{zR}^* \\ (\mathcal{E}_R^* + P_R^*) S_M \end{pmatrix} = S_R \begin{pmatrix} \rho_R \\ \rho_R v_{xR} \\ \rho_R v_{yR} \\ \rho_R v_{zR} \\ \mathcal{E}_R \end{pmatrix} - \begin{pmatrix} \rho_R v_{xR} \\ \rho_R v_{xR} v_{xR} + P_R \\ \rho_R v_{xR} v_{yR} \\ \rho_R v_{xR} v_{zR} \\ (\mathcal{E}_R + P_R) v_{xR} \end{pmatrix}
$$

First Row gives: $\rho_L^* = \rho_L \dfrac{S_L - v_{xL}}{S_L - S_M}$; $\rho_R^* = \rho_R \dfrac{S_R - v_{xR}}{S_R - S_M}$; Notice $\rho_L^* \neq \rho_R^*$. Why is that good?

Second Row yields constancy of pressure: $P^* = P_L^* = P_L + \rho_L (S_L - v_{xL})(S_M - v_{xL})$

$$= P_R^* = P_R + \rho_R (S_R - v_{xR})(S_M - v_{xR})$$

Third and fourth rows give constancy of transverse velocity:

$$v^*_{yL} = v_{yL} \quad ; \quad v^*_{yR} = v_{yR} \quad ; \quad v^*_{zL} = v_{zL} \quad ; \quad v^*_{zR} = v_{zR}$$

Fifth row gives the total energy density:

$$\mathcal{E}^*_L = \frac{(S_L - v_{xL})\mathcal{E}_L - P_L\, v_{xL} + P^*\, S_M}{S_L - S_M} \quad ; \quad \mathcal{E}^*_R = \frac{(S_R - v_{xR})\mathcal{E}_R - P_R\, v_{xR} + P^*\, S_M}{S_R - S_M}$$

$\mathcal{E}^*_L$ and $\mathcal{E}^*_R$ are formal entities . Their derivation is purely based on a formal jump condition. Don't ever use them to derive a "pressure".

The HLLC Riemann solver inherits all the same good properties that we catalogued for its progenitor HLL Riemann solver. Thus it too will:
1) represent *isolated shocks exactly*.
2) Have a *built-in entropy fix* for transonic rarefactions.
3) Make any scheme that uses it *positively conservative* in 1D (not 2D/3D).
4) It does its HLL parent one better *representing isolated contact discontinuities exactly*. It is also almost as fast as the HLL Riemann solver

HLLI Riemann Solver (Philosophy:- Start with HLL & build on top of it)

The HLLC RS is a decided improvement over the HLL RS, because it restores the contact discontinuity.

But notice that we had to work very hard to derive the HLLC RS; and it *only* restores the contact discontinuity.

What if we had several waves in a Riemann fan that we wanted to preserve crisply? One option would be to restore multiple discontinuities into an HLL RS. From our study of the HLLC RS, we realize that this would be a lot of work.

Another option, suggested by Einfeldt and Munz (hence the "EM"), would be to introduce a linear profile within HLL.

Intuitively, the right kind of profile would make more of the waves of interest flow in a particular direction, thereby reducing the dissipation of that wave family. Key benefit:- We can improve *any set* of wave families!

Intuitively speaking, realize that the Linearized RS and HLLC RS also reduce dissipation by introducing sub-structure in the Riemann fan. We build on that idea.

From the linearized RS, we realize that is should be related in some form to the characteristic weight :- $\alpha^p = l^p \cdot (U_R - U_L)$.

The real questions are:- What form of linear profile is optimal? And, how much of that profile is needed to exactly cancel the excessive dissipation from the HLL RS?

The details have been worked out in Dumbser & Balsara (2016).

The formulation works for hyperbolic systems in conservative or non-conservative form.

Key idea is to exploit the self-similarity of the Riemann fan. As a result, we develop the idea in self-similarity variables.

Typically, we start with $\dfrac{\partial U(x,t)}{\partial t} + \dfrac{\partial F(x,t)}{\partial x} = 0$

For special situations where the PDE system is indeed evolving self-similarly, we can write the problem in terms of the self-similarity variable $\xi = x/t$.

We can then write :- $U(x,t) = \tilde{U}(\xi)$; $F(x,t) = \tilde{F}(\xi)$.

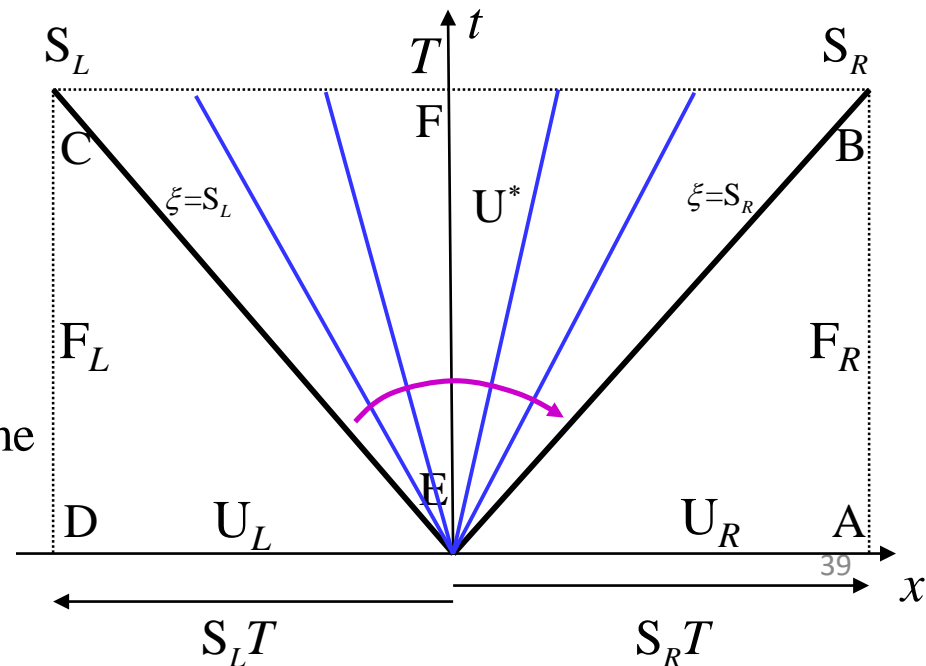$$\frac{\partial}{\partial t} = \frac{\partial \xi}{\partial t}\frac{\partial}{\partial \xi} = -\frac{\xi}{t^2}\frac{\partial}{\partial \xi} \qquad ; \qquad \frac{\partial}{\partial x} = \frac{\partial \xi}{\partial x}\frac{\partial}{\partial \xi} = \frac{1}{t}\frac{\partial}{\partial \xi}$$

$$\frac{\partial U(x,t)}{\partial t} + \frac{\partial F(x,t)}{\partial x} = 0$$

$\Rightarrow$

$$-\xi\frac{\partial \tilde{U}(\xi)}{\partial \xi} + \frac{\partial \tilde{F}(\xi)}{\partial \xi} = 0$$

Realize that "ξ" parametrizes various space-time points in the space-time diagram, going from $\xi = S_L$ on the left to $\xi = S_R$ on the right.

39

For HLL RS we can write

$$U_{HLL}^{(RS)}(\xi) = \begin{cases} U_L & \text{if } \xi < S_L \\ U^* & \text{if } S_L \leq \xi \leq S_R \\ U_R & \text{if } S_R < \xi \end{cases} \quad \text{with} \quad U^* = \frac{S_R U_R - S_L U_L - (F_R - F_L)}{S_R - S_L}$$

For HLLI RS we can improve the sharpness of the pth wave by writing the linear profile as:-

$$U_{HLLI}^{(RS)}(\xi) = \begin{cases} U_L & \text{if } \xi < S_L \\ U^* + 2\,\delta^p\,r^p \left[l^p (U_R - U_L) \right] \dfrac{\left(\xi - (S_R + S_L)/2 \right)}{(S_R - S_L)} & \text{if } S_L \leq \xi \leq S_R \\ U_R & \text{if } S_R < \xi \end{cases}$$

Recall that U^* is still the HLL state in the above formula.

If there are multiple waves that we want to improve (like contact + shear waves for Euler flow) or (like contact + Alfven waves for MHD flow) just add the contributions of those waves additively to the linear profile.

To make this work out just right (so that the dissipation is held to a minimum), we have to specify the scalar δ^p appropriately for each wave family. We do that next.

$$F_{HLLI}^{(RS)}(\xi) = \begin{cases} F_L & \text{if } 0 < S_L \\ F^* - \dfrac{S_R S_L}{(S_R - S_L)} \; \delta^p \; r^p \left[l^p (U_R - U_L) \right] & \text{if } S_L \leq 0 \leq S_R \\ F_R & \text{if } S_R < 0 \end{cases}$$

Recall that F^* is still the HLL flux in the above formula.

If there are multiple waves that we want to improve just add the contributions of those waves additively to the linear profile.

The HLLI Riemann solver is fully specified by setting the coefficient δ^p for the pth wave as:-

$$\delta^p = 1 - \frac{\min(\lambda^p, 0)}{S_L} - \frac{\max(\lambda^p, 0)}{S_R}$$

1) Just like the HLL RS, the HLLI RS does not require any further entropy fix.
2) Just like the HLL RS, the HLLI RS has good positivity enforcement properties.
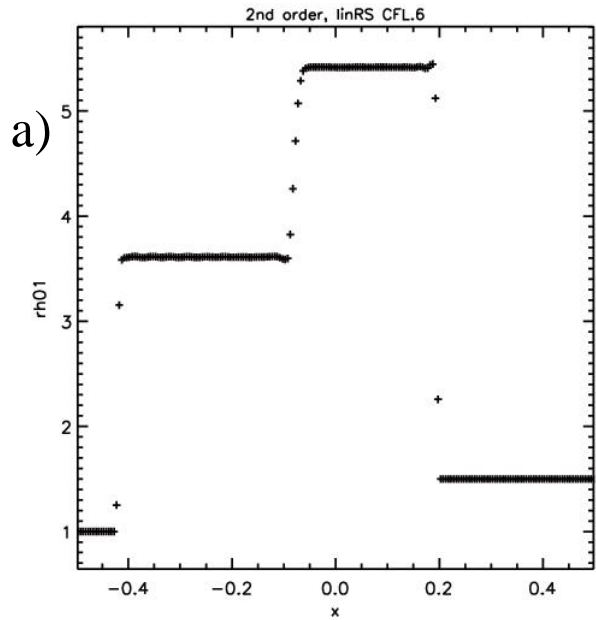3) HLLI improves over HLLC/HLLD because multiple intermediate waves can be steepened.

6.5.3) LLF Riemann Solver

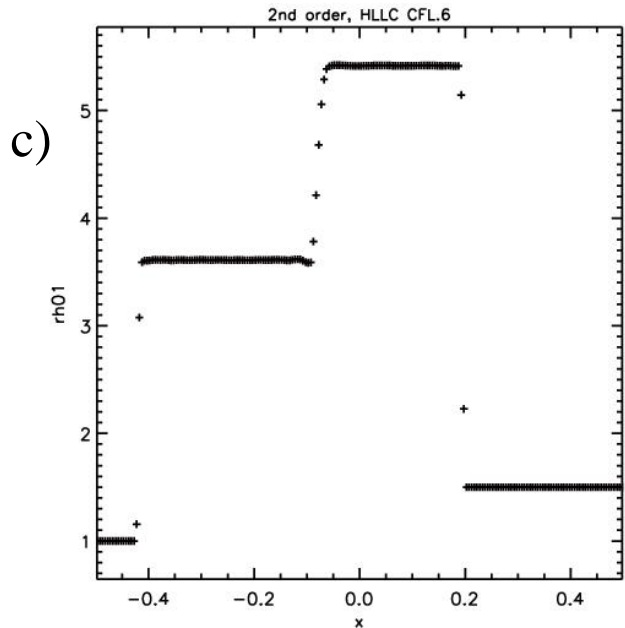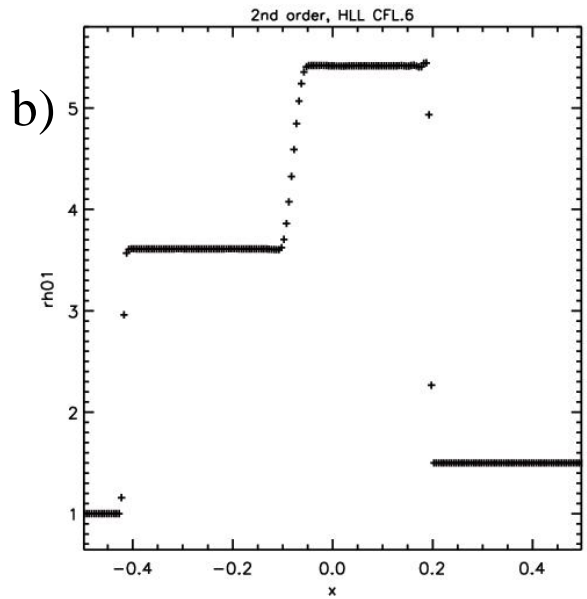Like before, it is based on taking the extremal speeds in the HLL Riemann solver to get:

$$S_{Max} \equiv \max\left(\left|\lambda^1\left(U_L\right)\right|, \left|\overline{v}_x - \overline{c}_s\right|, \left|\overline{v}_x + \overline{c}_s\right|, \left|\lambda^M\left(U_R\right)\right|\right) \quad ; \quad S_R = -S_L = S_{Max}$$

$$F_{LLF}^{(RS)} = \frac{1}{2}\left(F_L + F_R\right) - \frac{S_{Max}}{2}\left(U_R - U_L\right)$$
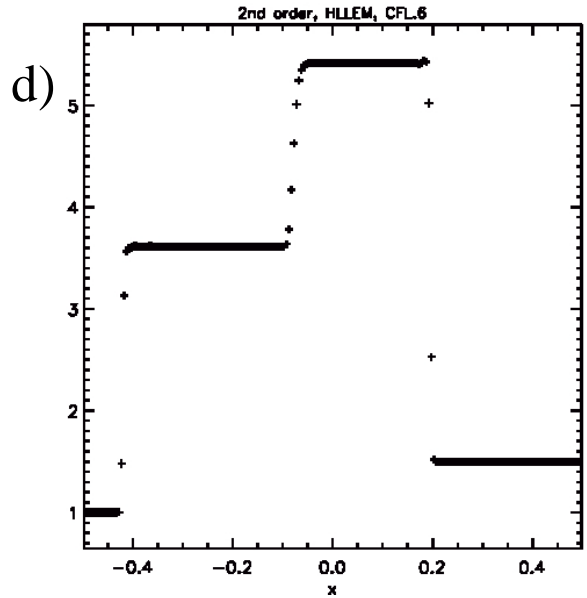
6.6) Intercomparing Riemann Solvers for the Euler Equations

Question: What differences do you see in the density profiles below?

a) 2nd order, linRS CFL.6

b) 2nd order, HLL CFL.6

← Roe

HLL →

c) 2nd order, HLLC CFL.6

d) 2nd order, HLLEM, CFL.6

← HLLC

HLLI →

6.7) Eigensystem for Non-Relativistic MHD

Can be written in a conservation form as:

$$\frac{\partial}{\partial t}\begin{pmatrix} \rho \\ \rho\, v_x \\ \rho\, v_y \\ \rho\, v_z \\ \mathcal{E} \\ B_x \\ B_y \\ B_z \end{pmatrix} + \frac{\partial}{\partial x}\begin{pmatrix} \rho\, v_x \\ \rho\, v_x^2 + P + \mathbf{B}^2/8\pi - B_x^2/4\pi \\ \rho\, v_x\, v_y - B_x\, B_y/4\pi \\ \rho\, v_x\, v_z - B_x\, B_z/4\pi \\ \left(\mathcal{E}+P+\mathbf{B}^2/8\pi\right)v_x - B_x\left(\mathbf{v}\cdot\mathbf{B}\right)/4\pi \\ 0 \\ \left(v_x\, B_y - v_y\, B_x\right) \\ -\left(v_z\, B_x - v_x\, B_z\right) \end{pmatrix}$$

Note the anisotropic pressures. Also note the magnetic tension terms.

$$+ \frac{\partial}{\partial y}\begin{pmatrix} \rho\, v_y \\ \rho\, v_x\, v_y - B_x\, B_y/4\pi \\ \rho\, v_y^2 + P + \mathbf{B}^2/8\pi - B_y^2/4\pi \\ \rho\, v_y\, v_z - B_y\, B_z/4\pi \\ \left(\mathcal{E}+P+\mathbf{B}^2/8\pi\right)v_y - B_y\left(\mathbf{v}\cdot\mathbf{B}\right)/4\pi \\ -\left(v_x\, B_y - v_y\, B_x\right) \\ 0 \\ \left(v_y\, B_z - v_z\, B_y\right) \end{pmatrix} + \frac{\partial}{\partial z}\begin{pmatrix} \rho\, v_z \\ \rho\, v_x\, v_z - B_x\, B_z/4\pi \\ \rho\, v_y\, v_z - B_y\, B_z/4\pi \\ \rho\, v_z^2 + P + \mathbf{B}^2/8\pi - B_z^2/4\pi \\ \left(\mathcal{E}+P+\mathbf{B}^2/8\pi\right)v_z - B_z\left(\mathbf{v}\cdot\mathbf{B}\right)/4\pi \\ \left(v_z\, B_x - v_x\, B_z\right) \\ -\left(v_y\, B_z - v_z\, B_y\right) \\ 0 \end{pmatrix} = 0$$

First 5 rows represent conservation of mass, momentum & energy. Last 3 represent the induction eqn.: $\dfrac{\partial \mathbf{B}}{\partial t} + c\,\nabla\times\mathbf{E} = 0$; $\mathbf{E} = -\dfrac{1}{c}\,\mathbf{v}\times\mathbf{B}$

With the constraint $\nabla \cdot \mathbf{B} = 0$, the induction equation ensures that if it is satisfied at the beginning of a calculation, it will be satisfied for all time.

$\nabla \cdot \mathbf{B} \neq 0$ results in unphysical plasma transport orthogonal to the field.

In a later chapter we will see how the constraint is imposed at a discrete level in a numerical code.

For x-directional variations, it ensures that B_x is constant.

$$
A = \begin{pmatrix}
0 & 1 & 0 & 0 & 0 & 0 & 0 \\[2mm]
-v_x^2 + \dfrac{(\Gamma-1)}{2}\mathbf{v}^2 & 2v_x - (\Gamma-1)v_x & -(\Gamma-1)v_y & -(\Gamma-1)v_z & (\Gamma-1) & (2-\Gamma)\dfrac{B_y}{4\pi} & (2-\Gamma)\dfrac{B_z}{4\pi} \\[2mm]
-v_x v_y & v_y & v_x & 0 & 0 & -\dfrac{B_x}{4\pi} & 0 \\[2mm]
-v_x v_z & v_z & 0 & v_x & 0 & 0 & -\dfrac{B_x}{4\pi} \\[2mm]
\delta_{51} & \delta_{52} & \delta_{53} & \delta_{54} & \delta_{55} & \delta_{56} & \delta_{57} \\[2mm]
-\dfrac{1}{\rho}\left(B_y v_x - B_x v_y\right) & \dfrac{B_y}{\rho} & -\dfrac{B_x}{\rho} & 0 & 0 & v_x & 0 \\[2mm]
-\dfrac{1}{\rho}\left(B_z v_x - B_x v_z\right) & \dfrac{B_z}{\rho} & 0 & -\dfrac{B_x}{\rho} & 0 & 0 & v_x
\end{pmatrix}
$$

Using the vector of primitive variables, $V \equiv \begin{pmatrix} \rho & v_x & v_y & v_z & P & B_y & B_z \end{pmatrix}^T$

we can write the hyperbolic system as $\partial_t V + A_p \ \partial_x V = 0$ with :

$$A_p = \begin{pmatrix} v_x & \rho & 0 & 0 & 0 & 0 & 0 \\ 0 & v_x & 0 & 0 & \dfrac{1}{\rho} & \dfrac{B_y}{4\pi\rho} & \dfrac{B_z}{4\pi\rho} \\ 0 & 0 & v_x & 0 & 0 & -\dfrac{B_x}{4\pi\rho} & 0 \\ 0 & 0 & 0 & v_x & 0 & 0 & -\dfrac{B_x}{4\pi\rho} \\ 0 & \rho c_s^2 & 0 & 0 & v_x & 0 & 0 \\ 0 & B_y & -B_x & 0 & 0 & v_x & 0 \\ 0 & B_z & 0 & -B_x & 0 & 0 & v_x \end{pmatrix}$$

Define the Alfvenic speeds as (They are useful for defining the wave speeds.)

$$b_x \equiv \frac{B_x}{\sqrt{4\pi\rho}} \ ; \ b_y \equiv \frac{B_y}{\sqrt{4\pi\rho}} \ ; \ b_z \equiv \frac{B_z}{\sqrt{4\pi\rho}} \ ; \ b \equiv \sqrt{b_x^2 + b_y^2 + b_z^2} \ ; \ b_\perp \equiv \sqrt{b_y^2 + b_z^2}$$

The wave speeds form an ordered set given by:

$$\{ v_x - m_f, \quad v_x - b_x, \quad v_x - m_s, \quad v_x, \quad v_x + m_s, \quad v_x + b_x, \quad v_x + m_f \}$$

To get m_f and m_s, solve the quartic : $m^4 - \left(c_s^2 + b^2 \right) m^2 + c_s^2 b_x^2 = 0$

Here m_f and m_s are the *fast and slow magnetosonic wave* speeds ($m_f \geq m_s \geq 0$)

It is important to learn the nomenclature of the waves, see fig. below:

Questions: Compare and contrast entropy waves in MHD and Euler flow.

Which waves take the place of shear waves? Are magnetosonic waves compressive?

Which waves are the analogues of sound waves? As $B_x \rightarrow 0$, which waves go to 0?
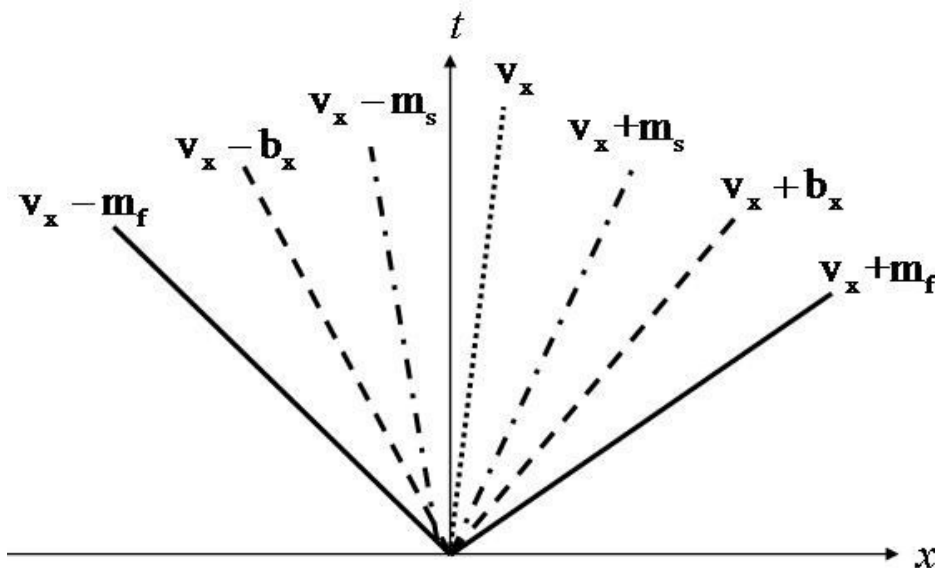
Fig. 6.4 shows the seven waves for the MHD system. They foliate symmetrically about the fluid's x-velocity. The fast waves are shown by solid lines. The Alfven waves are shown by dashed lines. The slow waves are shown by the dot-dashed lines. The entropy wave is shown by the dotted line.

The magnetic field breaks the degeneracy of the problem. Unlike sound waves, MHD waves do not propagate isotropically relative to the fluid's rest frame.

The wave propagation diagrams show B increasing from a) through c). <u>Question</u>: What do you see? Interpret the wave diagrams.
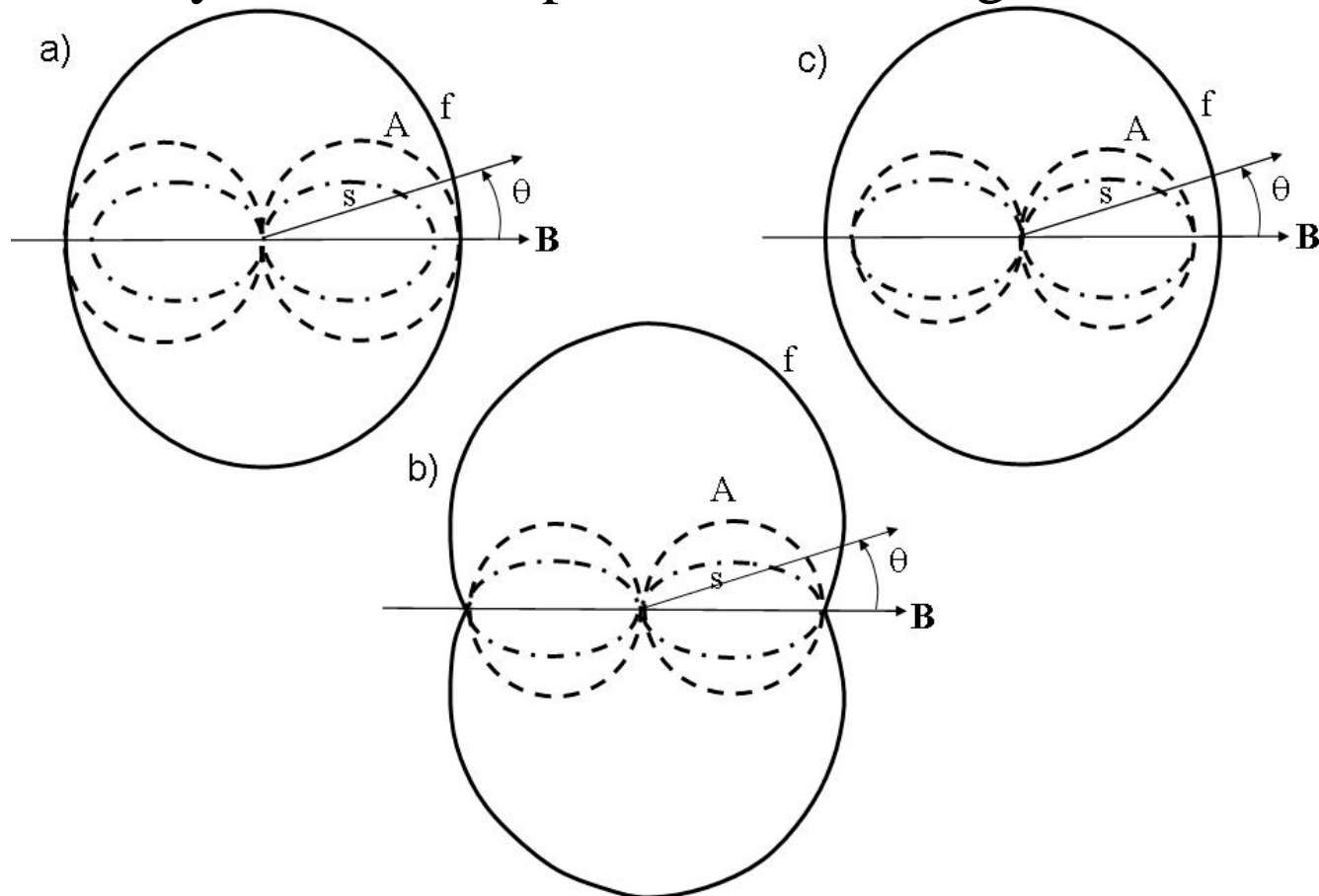
Fig. 6.5 showing surfaces of normal speeds for a) $b/c_s < 1$, b) $b/c_s = 1$, c) $b/c_s > 1$. The solid, dashed and dot-dashed curves show the fast, Alfven and slow wave speeds.

Eigenvalues become degenerate ➜ eigenvectors become indeterminate.

The indeterminacy is multiplicative and can be treated. This yields an eigenvector set that is orthonormal and salient in all the limits seen above (Roe & Balsara 1996).

Have to pay careful attention to the coefficients in all the limits.

$$
R_p = \begin{pmatrix}
\alpha_f\ \rho & 0 & \alpha_s\ \rho & 1 & \alpha_s\ \rho & 0 & \alpha_f\ \rho \\
-\alpha_f\ m_f & 0 & -\alpha_s\ m_s & 0 & \alpha_s\ m_s & 0 & \alpha_f\ m_f \\
\alpha_s\ m_s\ \beta_{y,s} & -\beta_z & -\alpha_f\ m_f\ \beta_{y,s} & 0 & \alpha_f\ m_f\ \beta_{y,s} & \beta_z & -\alpha_s\ m_s\ \beta_{y,s} \\
\alpha_s\ m_s\ \beta_{z,s} & \beta_y & -\alpha_f\ m_f\ \beta_{z,s} & 0 & \alpha_f\ m_f\ \beta_{z,s} & -\beta_y & -\alpha_s\ m_s\ \beta_{z,s} \\
\alpha_f\ \rho\ c_s^2 & 0 & \alpha_s\ \rho\ c_s^2 & 0 & \alpha_s\ \rho\ c_s^2 & 0 & \alpha_f\ \rho\ c_s^2 \\
\alpha_s\ \sqrt{4\pi\rho}\ c_s\ \beta_y & -\sqrt{4\pi\rho}\,\beta_{z,s} & -\alpha_f\ \sqrt{4\pi\rho}\ c_s\ \beta_y & 0 & -\alpha_f\ \sqrt{4\pi\rho}\ c_s\ \beta_y & -\sqrt{4\pi\rho}\,\beta_{z,s} & \alpha_s\ \sqrt{4\pi\rho}\ c_s\ \beta_y \\
\alpha_s\ \sqrt{4\pi\rho}\ c_s\ \beta_z & \sqrt{4\pi\rho}\,\beta_{y,s} & -\alpha_f\ \sqrt{4\pi\rho}\ c_s\ \beta_z & 0 & -\alpha_f\ \sqrt{4\pi\rho}\ c_s\ \beta_z & \sqrt{4\pi\rho}\,\beta_{y,s} & \alpha_s\ \sqrt{4\pi\rho}\ c_s\ \beta_z
\end{pmatrix}
$$

6.8) Linearized Riemann Solver for the MHD Equations

We define the Roe-averaged magnetic fields differently, retaining the original definitions of the velocities etc.

$$\underline{B}_y \equiv \frac{\sqrt{\rho_R}\,B_{yL} + \sqrt{\rho_L}\,B_{yR}}{\sqrt{\rho_L} + \sqrt{\rho_R}} \quad ; \quad \underline{B}_z \equiv \frac{\sqrt{\rho_R}\,B_{zL} + \sqrt{\rho_L}\,B_{zR}}{\sqrt{\rho_L} + \sqrt{\rho_R}}$$

This allows us to derive (after a lot of symbolic manipulation)

$$\Delta\left(\frac{\mathbf{B}^2}{2}\right) = X\,\Delta\rho + \underline{\mathbf{B}} \cdot \Delta\mathbf{B} \quad ; \quad X \equiv \frac{\left(\Delta\mathbf{B}\right)^2}{2\left(\sqrt{\rho_L} + \sqrt{\rho_R}\right)^2}$$

$$\Delta P = \left(\Gamma - 1\right)\left[\left(\frac{\overline{\mathbf{v}}^2}{2} - \frac{X}{4\pi}\right)\Delta\rho - \overline{\mathbf{v}} \cdot \Delta\left(\rho\,\overline{\mathbf{v}}\right) + \Delta\mathcal{E} - \frac{1}{4\pi}\,\underline{\mathbf{B}} \cdot \Delta\mathbf{B}\right]$$

Manipulations similar to those for the Euler equations allow us to obtain a formal similarity to the actual, physical, characteristic matrix:

$$\bar{A} = \begin{pmatrix}
0 & 1 & 0 & 0 & 0 & 0 & 0 \\
-\bar{v}_x^2 + \frac{(\Gamma-1)}{2}\bar{\mathbf{v}}^2 + (2-\Gamma)\frac{X}{4\pi} & 2\bar{v}_x - (\Gamma-1)\bar{v}_x & -(\Gamma-1)\bar{v}_y & -(\Gamma-1)\bar{v}_z & (\Gamma-1) & (2-\Gamma)\frac{B_y}{4\pi} & (2-\Gamma)\frac{B_z}{4\pi} \\
-\bar{v}_x\bar{v}_y & \bar{v}_y & \bar{v}_x & 0 & 0 & -\frac{B_x}{4\pi} & 0 \\
-\bar{v}_x\bar{v}_z & \bar{v}_z & 0 & \bar{v}_x & 0 & 0 & -\frac{B_x}{4\pi} \\
\bar{\delta}_{51} & \bar{\delta}_{52} & \bar{\delta}_{53} & \bar{\delta}_{54} & \bar{\delta}_{55} & \bar{\delta}_{56} & \bar{\delta}_{57} \\
-\frac{1}{\rho^*}\left(\underline{B}_y\bar{v}_x - B_x\bar{v}_y\right) & \frac{B_y}{\rho^*} & -\frac{B_x}{\rho^*} & 0 & 0 & \bar{v}_x & 0 \\
-\frac{1}{\rho^*}\left(\underline{B}_z\bar{v}_x - B_x\bar{v}_z\right) & \frac{B_z}{\rho^*} & 0 & -\frac{B_x}{\rho^*} & 0 & 0 & \bar{v}_x
\end{pmatrix}$$

Recall the Euler case. Familiar extensions to the definition of the sound speed follow:

$$\bar{c}_s^2 = \frac{\Gamma\,\bar{P}}{\rho^*} \quad ; \quad \bar{P} \equiv \frac{(\Gamma-1)}{\Gamma}\rho^*\left(\bar{H} - \frac{\bar{\mathbf{v}}^2}{2} - \frac{\underline{\mathbf{B}}^2}{4\pi\rho^*}\right) - \frac{(\Gamma-2)}{\Gamma}\rho^*\frac{X}{4\pi}$$

Analogous definitions for the Alfvenic speeds can also be obtained:

$$\bar{b}_x \equiv \frac{B_x}{\sqrt{4\pi\rho^*}} \quad ; \quad \bar{b}_y \equiv \frac{B_y}{\sqrt{4\pi\rho^*}} \quad ; \quad \bar{b}_z \equiv \frac{B_z}{\sqrt{4\pi\rho^*}} \quad ; \quad \bar{b} \equiv \sqrt{\bar{b}_x^2 + \bar{b}_y^2 + \bar{b}_z^2} \quad ; \quad \bar{b}_\perp \equiv \sqrt{\bar{b}_y^2 + \bar{b}_z^2}$$

The ordered set of analogous eigenvalues are given by:

$$\left\{ \overline{v}_x - \overline{m}_f, \quad \overline{v}_x - \overline{b}_x, \quad \overline{v}_x - \overline{m}_s, \quad \overline{v}_x, \quad \overline{v}_x + \overline{m}_s, \quad \overline{v}_x + \overline{b}_x, \quad \overline{v}_x + \overline{m}_f \right\}$$

and they are obtained from the analogous quartic:

$$\overline{m}^4 - \left(\overline{c}_s^2 + \overline{b}^2 \right) \overline{m}^2 + \overline{c}_s^2 \, \overline{b}_x^2 = 0$$

We can also obtain the analogous eigenvectors:

$$R_p = \begin{pmatrix} \overline{\alpha}_f \, \rho^* & 0 & \overline{\alpha}_s \, \rho^* & 1 & \overline{\alpha}_s \, \rho^* & 0 & \overline{\alpha}_f \, \rho^* \\ -\overline{\alpha}_f \, \overline{m}_f & 0 & -\overline{\alpha}_s \, \overline{m}_s & 0 & \overline{\alpha}_s \, \overline{m}_s & 0 & \overline{\alpha}_f \, \overline{m}_f \\ \overline{\alpha}_s \, \overline{m}_s \, \overline{\beta}_{y,s} & -\overline{\beta}_z & -\overline{\alpha}_f \, \overline{m}_f \, \overline{\beta}_{y,s} & 0 & \overline{\alpha}_f \, \overline{m}_f \, \overline{\beta}_{y,s} & \overline{\beta}_z & -\overline{\alpha}_s \, \overline{m}_s \, \overline{\beta}_{y,s} \\ \overline{\alpha}_s \, \overline{m}_s \, \overline{\beta}_{z,s} & \overline{\beta}_y & -\overline{\alpha}_f \, \overline{m}_f \, \overline{\beta}_{z,s} & 0 & \overline{\alpha}_f \, \overline{m}_f \, \overline{\beta}_{z,s} & -\overline{\beta}_y & -\overline{\alpha}_s \, \overline{m}_s \, \overline{\beta}_{z,s} \\ \overline{\alpha}_f \, \rho^* \left(\overline{c}_s^2 - \dfrac{X}{4\pi} \right) & 0 & \overline{\alpha}_s \, \rho^* \left(\overline{c}_s^2 - \dfrac{X}{4\pi} \right) & -\dfrac{X}{4\pi} & \overline{\alpha}_s \, \rho^* \left(\overline{c}_s^2 - \dfrac{X}{4\pi} \right) & 0 & \overline{\alpha}_f \, \rho^* \left(\overline{c}_s^2 - \dfrac{X}{4\pi} \right) \\ \overline{\alpha}_s \, \sqrt{4\pi\rho^*} \, \overline{c}_s \, \overline{\beta}_y & -\sqrt{4\pi\rho^*}\, \overline{\beta}_{z,s} & -\overline{\alpha}_f \, \sqrt{4\pi\rho^*} \, \overline{c}_s \, \overline{\beta}_y & 0 & -\overline{\alpha}_f \, \sqrt{4\pi\rho^*} \, \overline{c}_s \, \overline{\beta}_y & -\sqrt{4\pi\rho^*}\, \overline{\beta}_{z,s} & \overline{\alpha}_s \, \sqrt{4\pi\rho^*} \, \overline{c}_s \, \overline{\beta}_y \\ \overline{\alpha}_s \, \sqrt{4\pi\rho^*} \, \overline{c}_s \, \overline{\beta}_z & \sqrt{4\pi\rho^*}\, \overline{\beta}_{y,s} & -\overline{\alpha}_f \, \sqrt{4\pi\rho^*} \, \overline{c}_s \, \overline{\beta}_z & 0 & -\overline{\alpha}_f \, \sqrt{4\pi\rho^*} \, \overline{c}_s \, \overline{\beta}_z & \sqrt{4\pi\rho^*}\, \overline{\beta}_{y,s} & \overline{\alpha}_s \, \sqrt{4\pi\rho^*} \, \overline{c}_s \, \overline{\beta}_z \end{pmatrix}$$

We use the same *entropy fixes* as before.

There is some analysis to show that the effects of non-convexity are not severe.

We keep B_x constant across all these Riemann solvers.

The HLL and LLF Riemann solvers continue to have the same definitions. All that changes is the definitions of the extremal signal speeds:

For HLL we use:

$$S_L \equiv \min\left(\lambda^1\left(U_L\right), \overline{v}_x - \overline{m}_f, 0\right) \quad ; \quad S_R \equiv \max\left(\lambda^M\left(U_R\right), \overline{v}_x + \overline{m}_f, 0\right)$$

For LLF we use:

$$S_{Max} \equiv \max\left(\left|\lambda^1\left(U_L\right)\right|, \left|\overline{v}_x - \overline{m}_f\right|, \left|\overline{v}_x + \overline{m}_f\right|, \left|\lambda^M\left(U_R\right)\right|\right)$$

6.9.2) HLLD Riemann Solver for MHD

Recall : The Euler equations have one contact discontinuity. Restoring it in the HLL Riemann solver gave us the HLLC Riemann solver.

The MHD equations have three linearly degenerate waves : One *contact* discontinuity and two *Alfven waves*. Restoring these waves in the HLL Riemann solver gives us the **HLLD Riemann solver**. The "*D*" stands for these *discontinuities*.
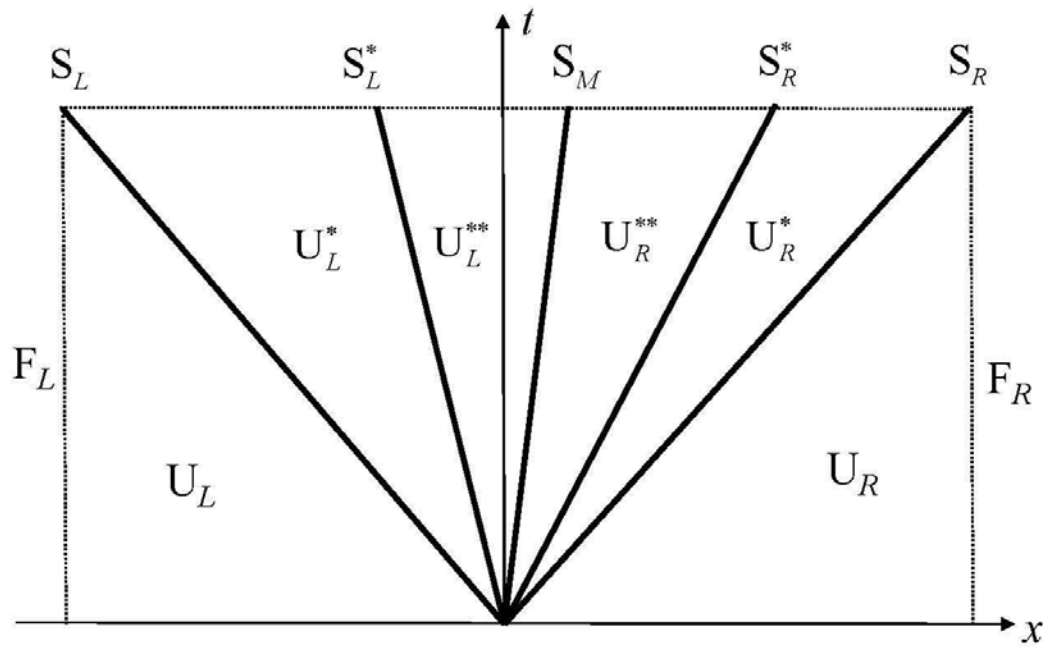
Fig. 6.6 is a schematic diagram showing the six constant states in the HLLD Riemann solver for MHD. The leftmost and rightmost waves are shown as S_L and S_R respectively. The contact discontinuity is shown as S_M. The left and right-going Alfven waves are shown as S_L^* and S_R^* respectively.

The HLLD Riemann solver uses the following wave model with 6 *constant states*:

$$
F_{HLLD}^{(RS)} = \begin{cases}
F_L & \text{if } S_L > 0 \\
F_L^* & \text{if } S_L \leq 0 \leq S_L^* \\
F_L^{**} & \text{if } S_L^* \leq 0 \leq S_M \\
F_R^{**} & \text{if } S_M \leq 0 \leq S_R^* \\
F_R^* & \text{if } S_R^* \leq 0 \leq S_R \\
F_R & \text{if } S_R < 0
\end{cases}
$$

S_M , S_L^* and S_R^* will correspond to the speed of the *contact discontinuity* and the *Alfven waves*. We will obtain S_M using a strategy that is similar to the Euler case.

1) The HLLD Riemann solver for MHD is also provably *positively conservative*.
2) Just like the HLL Riemann solver, it too has an *in-built entropy fix*.
3) Like the HLLC, it too will capture *isolated fast magnetosonic shocks exactly*. It does *average over* the *slow magnetosonic shocks*. However, the slow magnetosonic shocks can only support a small pressure jump, so their contribution to the overall discontinuity is not too large. Hence, it is ok to ignore them.

As with the HLLC Riemann solver, we wish to keep the total pressure constant across the contact discontinuity and Alfven waves:

$$P_T \equiv P + \frac{\mathbf{B}^2}{8\pi}$$

As with the HLLC Riemann solver, this is achieved by asserting that the x-component of the velocity is a constant across the Riemann fan:

$$S_M = v_{xL}^* = v_{xR}^* = v_{xL}^{**} = v_{xR}^{**} = \frac{\rho_R \, v_{xR}\left(S_R - v_{xR}\right) - \rho_L \, v_{xL}\left(S_L - v_{xL}\right) + P_{TL} - P_{TR}}{\rho_R\left(S_R - v_{xR}\right) - \rho_L\left(S_L - v_{xL}\right)}$$

As with the HLLC Riemann solver, the states U_L^* and U_R^* are obtained by writing jump conditions:

$$S_L \begin{pmatrix} \rho_L^* \\ \rho_L^* S_M \\ \rho_L^* v_{yL}^* \\ \rho_L^* v_{zL}^* \\ \varepsilon_L^* \\ B_{yL}^* \\ B_{zL}^* \end{pmatrix} - \begin{pmatrix} \rho_L^* S_M \\ \rho_L^* S_M^2 + P_{TL}^* - B_x^2/4\pi \\ \rho_L^* S_M v_{yL}^* - B_x B_{yL}^*/4\pi \\ \rho_L^* S_M v_{zL}^* - B_x B_{zL}^*/4\pi \\ \left(\varepsilon_L^* + P_{TL}^*\right)S_M - B_x\left(\mathbf{v}_L^* \cdot \mathbf{B}_L^*\right)/4\pi \\ B_{yL}^* S_M - B_x v_{yL}^* \\ B_{zL}^* S_M - B_x v_{zL}^* \end{pmatrix} = S_L \begin{pmatrix} \rho_L \\ \rho_L v_{xL} \\ \rho_L v_{yL} \\ \rho_L v_{zL} \\ \varepsilon_L \\ B_{yL} \\ B_{zL} \end{pmatrix} - \begin{pmatrix} \rho_L v_{xL} \\ \rho_L v_{xL}^2 + P_{TL} - B_x^2/4\pi \\ \rho_L v_{xL} v_{yL} - B_x B_{yL}/4\pi \\ \rho_L v_{xL} v_{zL} - B_x B_{zL}/4\pi \\ \left(\varepsilon_L + P_{TL}\right)v_{xL} - B_x\left(\mathbf{v}_L \cdot \mathbf{B}_L\right)/4\pi \\ B_{yL} v_{xL} - B_x v_{yL} \\ B_{zL} v_{xL} - B_x v_{zL} \end{pmatrix}$$

56

The first row gives: $\rho_L^* = \rho_L \dfrac{S_L - v_{xL}}{S_L - S_M}$

The second row gives: $P_T^* = P_{TL}^* = P_{TL}^{**} = P_{TL} + \rho_L(S_L - v_{xL})(S_M - v_{xL})$

The third and sixth rows give: $v_{yL}^* = v_{yL} - \dfrac{B_x B_{yL}}{4\pi} \dfrac{S_M - v_{xL}}{\rho_L(S_L - v_{xL})(S_L - S_M) - B_x^2/4\pi}$;

and $\quad B_{yL}^* = B_{yL} \dfrac{\rho_L(S_L - v_{xL})^2 - B_x^2/4\pi}{\rho_L(S_L - v_{xL})(S_L - S_M) - B_x^2/4\pi}$

(Similar expressions are obtained from the 4th and 7th rows.)

The fifth row gives: $\mathcal{E}_L^* = \dfrac{(S_L - v_{xL})\mathcal{E}_L - P_{TL}\, v_{xL} + P_T^*\, S_M + B_x\left(\mathbf{v}_L \cdot \mathbf{B}_L - \mathbf{v}_L^* \cdot \mathbf{B}_L^*\right)/4\pi}{S_L - S_M}$

As with the HLLC Riemann solver, these expressions are based on a formal analogy.

The Alfven wave speeds are written by analogy: $S_L^* = S_M - \dfrac{|B_x|}{\sqrt{4\pi\rho_L^*}}$; $S_R^* = S_M + \dfrac{|B_x|}{\sqrt{4\pi\rho_R^*}}$

The jump conditions across the contact discontinuity give the expected results:

$$P_{TL}^{**} = P_{TR}^{**} \quad ; \quad v_{yL}^{**} = v_{yR}^{**} \quad ; \quad v_{zL}^{**} = v_{zR}^{**} \quad ; \quad B_{yL}^{**} = B_{yR}^{**} \quad ; \quad B_{zL}^{**} = B_{zR}^{**}$$

Asserting the formal jumps across the Alfven waves, unfortunately, does not give us as much insight as we wish. Nor does it give us clean expressions for all the U_L^{**} and U_R^{**} variables. We can only squeeze so much out of our analogies!

We get : $\rho_L^{**} = \rho_L^* \quad ; \quad P_{TL}^{**} = P_{TL}^* \quad ; \quad \mathcal{E}_L^{**} = \mathcal{E}_L^* - \sqrt{\rho_L^*}\left(\mathbf{v}_L^* \cdot \mathbf{B}_L^* - \mathbf{v}_L^{**} \cdot \mathbf{B}_L^{**}\right)\ \mathrm{sgn}(B_x)\big/\sqrt{4\pi}$

Lastly, integrating over the dotted rectangle in the previous space-time diagram gives:

$$v_{yL}^{**} = v_{yR}^{**} = \frac{\sqrt{\rho_L^*}\ v_{yL}^* + \sqrt{\rho_R^*}\ v_{yR}^* + \left(B_{yR}^* - B_{yL}^*\right)\ \mathrm{sgn}(B_x)\big/\sqrt{4\pi}}{\sqrt{\rho_L^*} + \sqrt{\rho_R^*}}\quad ;$$

$$B_{yL}^{**} = B_{yR}^{**} = \frac{\sqrt{\rho_L^*}\ B_{yR}^* + \sqrt{\rho_R^*}\ B_{yL}^* + \sqrt{\rho_L^*\rho_R^*}\left(v_{yR}^* - v_{yL}^*\right)\ \mathrm{sgn}(B_x)\sqrt{4\pi}}{\sqrt{\rho_L^*} + \sqrt{\rho_R^*}}$$

6.10) Riemann Problem for the MHD System

The result of the Riemann problem for the Euler system is easy to classify, not so for MHD, where over 200 outcomes are possible.

The system is *non-convex* and *non-strictly hyperbolic* ➔ wave families can intersect and form compound waves. A shock can be attached to a rarefaction wave, as we saw in Chapter 4.

Fast magnetosonic shocks *increase* the *transverse component* of the magnetic field. *Slow magnetosonic* shocks *decrease* the *transverse component* of the magnetic field. <u>Question</u>: Rarefaction fans act oppositely, so how are transverse fields treated by rarefaction fans?

This opens the door to *switch-on fast magnetosonic shocks* or *switch-on slow magnetosonic rarefactions*.

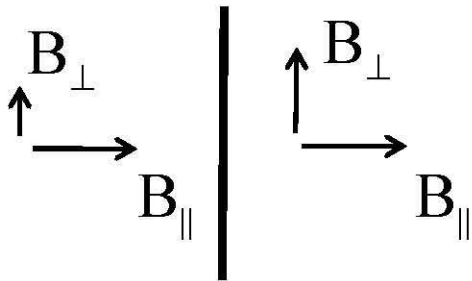Likewise, we can have *switch-off fast magnetosonic rarefactions* or *switch-off slow magnetosonic shocks*.
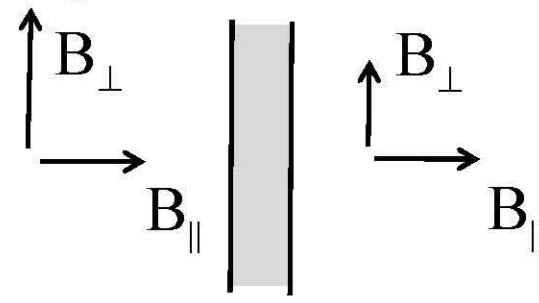
Right-going fast
magnetosonic shock
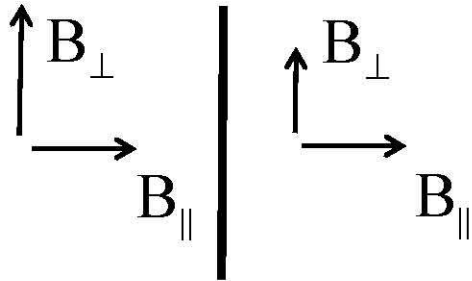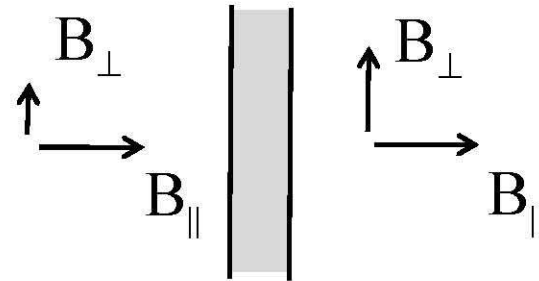
$B_\perp$

$B_\perp$

$B_\parallel$

$B_\parallel$

Right-going fast
magnetosonic rarefaction

$B_\perp$

$B_\perp$

$B_\parallel$

$B_\parallel$

Right-going slow
magnetosonic shock

$B_\perp$

$B_\perp$

$B_\parallel$

$B_\parallel$

Right-going slow
magnetosonic rarefaction

$B_\perp$

$B_\perp$

$B_\parallel$

$B_\parallel$

Figure 6.7 schematically displays the increasing or decreasing trends in the transverse magnetic field for right-going fast and slow magnetosonic shocks and right-going fast and slow magnetosonic rarefactions.

$$\left(\rho,\, P,\, v_x,\, v_y,\, v_z,\, B_y,\, B_z \right) = (\, 1,\, 1,\, 0,\, 0,\, 0,\, \sqrt{4\pi},\, 0) \qquad \text{for } x<0 \qquad \Gamma=2; \quad B_x = 0.75\,\sqrt{4\pi}$$

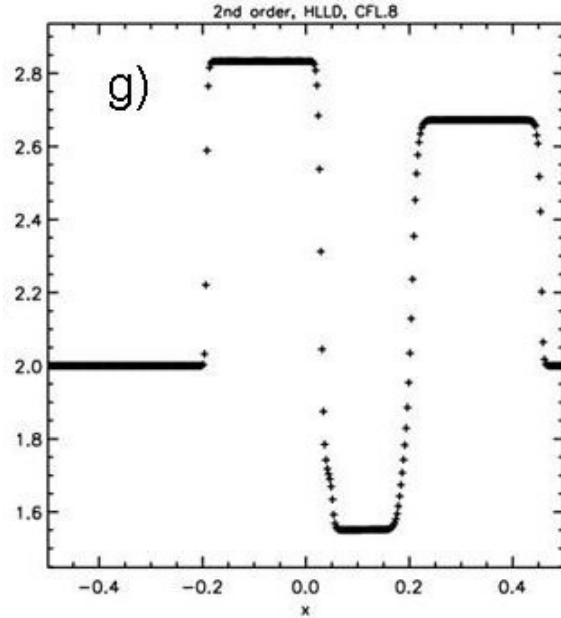$$= (\, 0.125,\, 0.1,\, 0,\, 0,\, 0,\, -\sqrt{4\pi},\, 0) \qquad \text{for } x>0$$
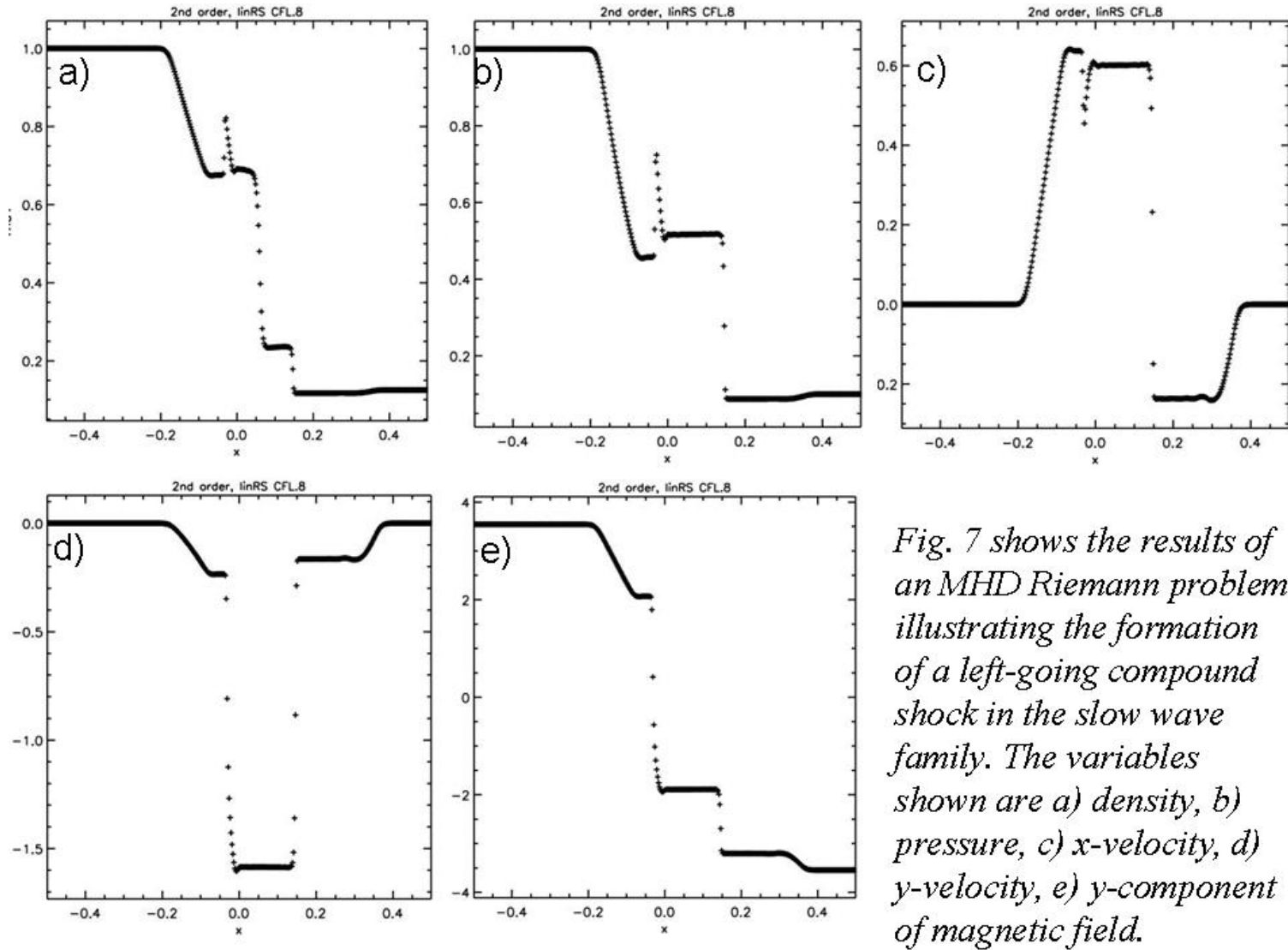
Fig. 7 shows the results of an MHD Riemann problem illustrating the formation of a left-going compound shock in the slow wave family. The variables shown are a) density, b) pressure, c) x-velocity, d) y-velocity, e) y-component of magnetic field.

The left-going slow compound wave is genuinely a consequence of the field reversal in a coplanar problem. If there were a non-coplanarity, it would not show up.

$$\left(\rho, P, v_x, v_y, v_z, B_y, B_z\right) = (1.08, 0.95, 1.2, 0.01, 0.5, 3.6, 2.0) \quad \text{for } x<0 \quad \Gamma=5/3; \quad B_x = 2$$

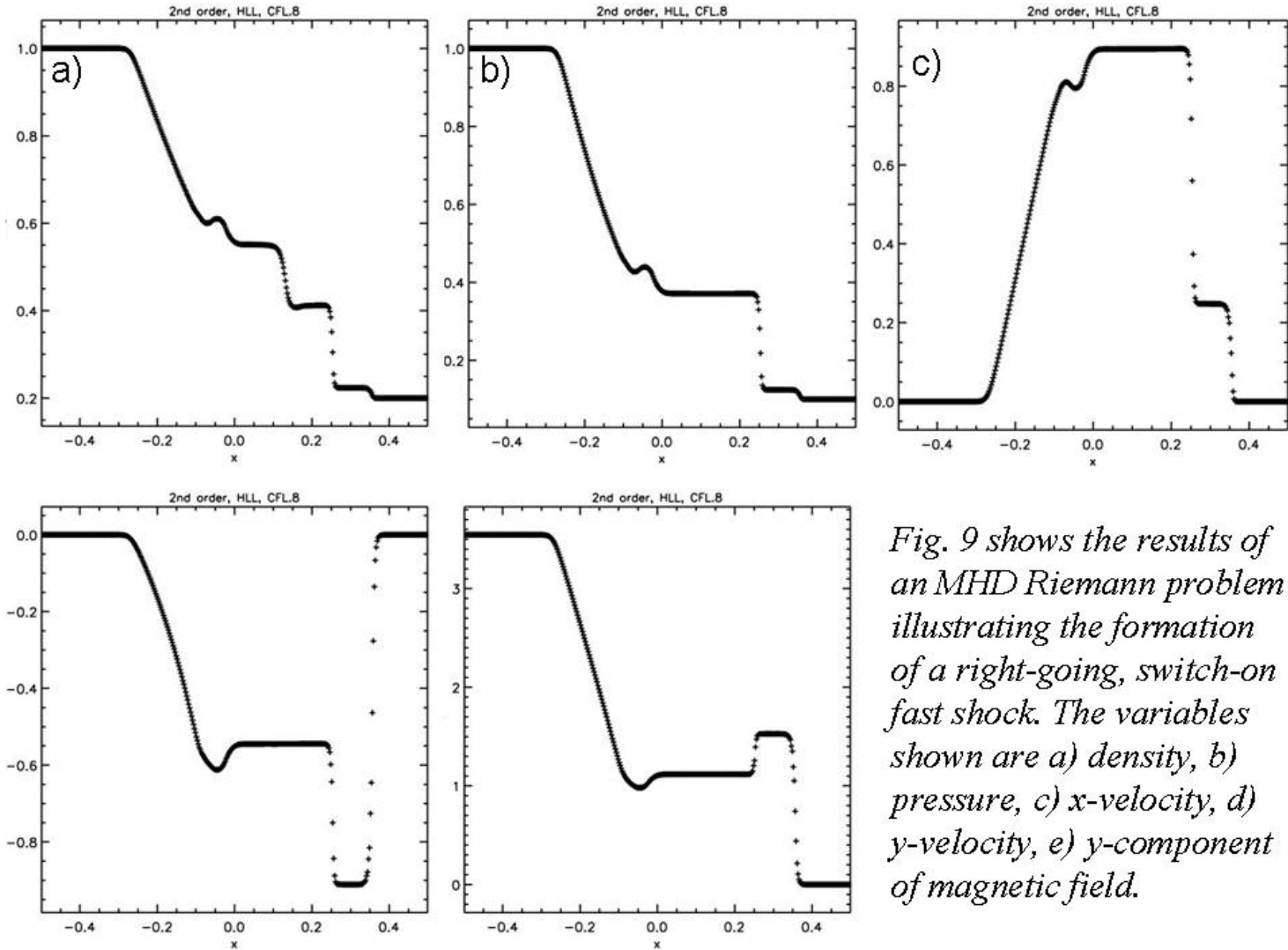$$= (1, 1, 0, 0, 0, 4, 2) \quad \text{for } x>0$$
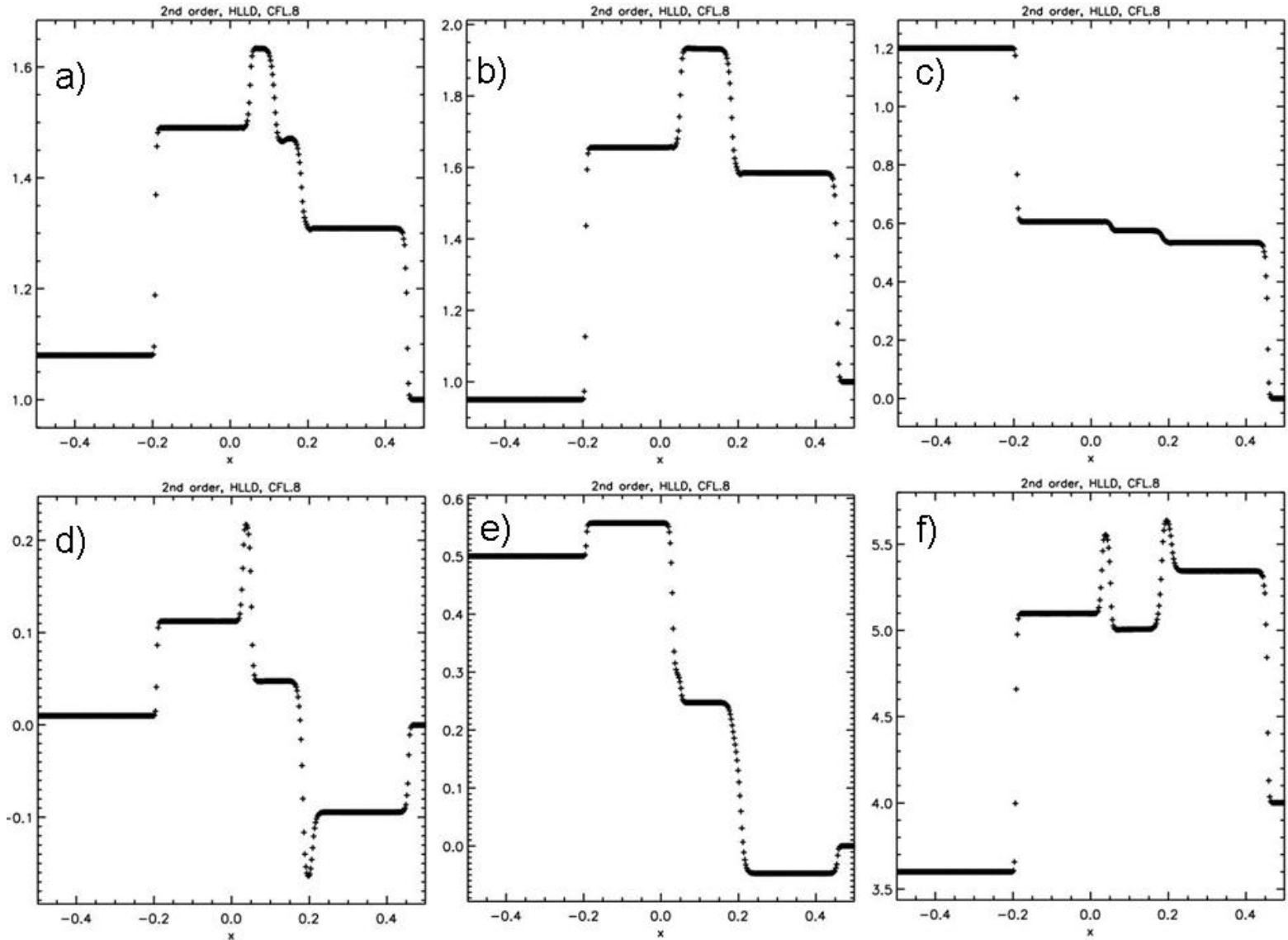
Fig. 8 shows the results of an MHD Riemann problem illustrating the formation of all seven families of waves. The variables shown are a) density, b) pressure, c) x-velocity, d) y-velocity, e) z-velocity, f) y-component of magnetic field and g) z-component of magnetic field.

$$\left(\rho, P, v_x, v_y, v_z, B_y, B_z \right) = (1, 1, 0, 0, 0, \sqrt{4\pi}, 0)$$

for x<0 Γ=5/3; $B_x = \sqrt{4\pi}$

$$= (0.2, 0.1, 0, 0, 0, 0, 0)$$
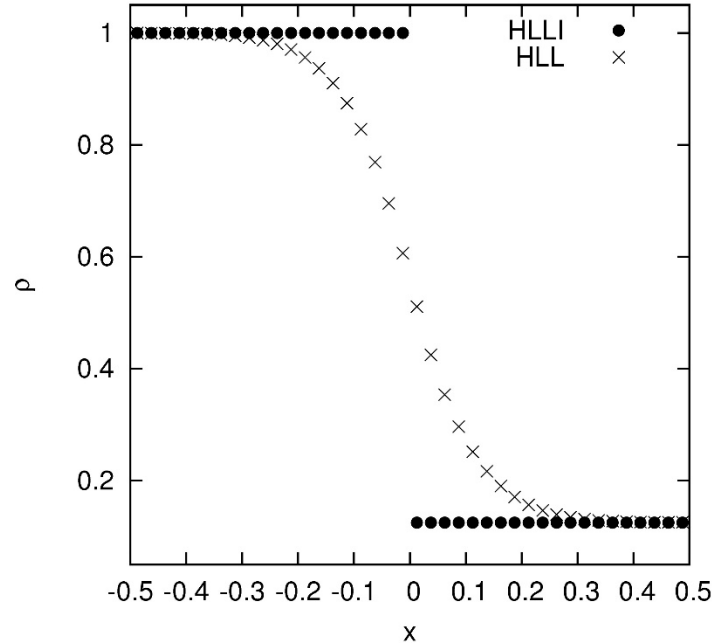
for x>0

Fig. 9 shows the results of an MHD Riemann problem illustrating the formation of a right-going, switch-on fast shock. The variables shown are a) density, b) pressure, c) x-velocity, d) y-velocity, e) y-component of magnetic field.

Right-going switch-on fast shock.

Preserving Stationary Contact Discontinuities (HLL v/s HLLI)

Preserving Stationary Alfven waves (HLL v/s HLLI)